


Stability Analysis of a Sterile Insect Technique Model for Controlling False Codling Moth

JIMRISE O. OCHWACH ^a , MARK O. OKONGO ^{a,*}, MOSES M. MURAYA ^b

^a Department of Physical Science, Chuka University, Chuka, Kenya

^b Department of Plant Science, Chuka University, Chuka, Kenyas

• Received: 13 August 2022

• Accepted: 28 June 2023

• Published Online: 30 June 2023

Abstract

Sterile insect techniques (SIT) are biological, non-polluting pest control methods used on farms. The release of false male codling moths (FCM) is used in this method to reduce the number of fertile female FCM in the farm population. In this study, a mathematical model that simulates the interaction between the susceptible host, the sterile male FCM population, and the wild FCM population is developed. The local and global stability analysis of the model is analysed and found to be asymptotically stable when $R_0 < 1$. A threshold number of sterile FCM is determined above which the FCM control is effective. These theoretical results are reorganised in terms of possible strategies for the control of FCM and are numerically illustrated.

Keywords: Sterile insect technique, Mathematical modelling, codling moth, Stability analysis, Plant pest model, pest control .

2010 MSC: Applied Mathematics, Epidemiology, Mathematical Modelling.

1. Introduction

Sterile Insect Technique (SIT) has been used successfully for more than half a century to eliminate or control many pest species, especially the dipteran [4]. This technique is a biological control method that prevents insect pests from reproducing naturally. This is achieved by treating male insect pests with chemical, physical, or other radical procedures to make them infertile, preventing them from reproducing regardless of their sex drive [6]. In SIT, sterile organisms mate with fertile organisms, leading to unproductive mating, thus controlling their population by reducing the number of viable offspring [14]. Consequently, this leads to the decline of the FCM population over time. Therefore, releasing sufficiently many sterile males into the wild FCM population over a sufficiently long period of time can lead to the reduction or elimination of FCM on a farm [32, 3]. This technique has given farmers the ability to control pests from certain insects in livestock,

*Jimrise O. Ochwach: ojimrise09@gmail.com

fruits, vegetables, and fibre crops. It is also an environmentally friendly approach, as it uses no noxious chemicals, leaves no residues, and is entirely species specific, thus having no non-target effects on crops and livestock [15].

However, in most SIT models, none has been used in the control of false codling moth (FCM). The main critical factors in pest control using SIT are the critical sterile release rate and the over-inundation ratio, which is the measure of the ratio of sterile males to wild males [38]. False codling moth (FCM), *Thaumatotibia leucotreta*, is considered the most significant indigenous pest [19]. This is due to its potential economic impact on many horticultural and agricultural crops [35, 19]. Consequently, FCM is a major threat to food security, the supply of raw materials for manufacturing, foreign exchange, and employment in many countries [9, 19].

Sterile release models were developed by [3] to control anopheles mosquitoes and [4] to determine the rate of sterile release. However, most of these mathematical models do not address the population dynamics of FCM, the control measure that this study seeks to address. Planning efficient and cost-effective control is a real challenge that can explain the failure of most experimental methods of the FCM control strategy [2]. This is because biological systems can become unstable or stable if certain parameters are changed appropriately, that is, if their values pass through bifurcation points [29, 37, 35]. Therefore, more scientific studies are needed on how changes such as SIT affect the biological system of host-pest relationships.

False codling moth (FCM), *Thaumatotibia leucotreta* is considered the most significant indigenous pest. This is due to its potential economic impact on many horticultural and agricultural crops, with crop losses ranging from 20 – 90% ([36]. Consequently, FCM is a major threat to food security, supply of raw material for manufacturing, foreign exchange and employment in many countries [10]. FCM is widely distributed across Africa and has been reported in over 40 Africa countries, including Kenya [39]. The FCM is not considered to be established outside of Africa. However, it is commonly intercepted during quarantine inspections in Europe and United States [18]. Therefore, FCM is a pest of phytosanitary concern and it impedes export in most international markets, as it is endemic to sub-Saharan Africa [20, 28]. Consequently, interception of even an individual pest in a consignment could lead to rejection of the entire consignment [28, 27].

After the adults mate, the female deposits eggs on fruit or foliage, either in batches or as single eggs. The eggs are hemispherical in shape with a granulated surface and translucent in color and appear cream to white when first laid [39]. The eggs are usually deposited on the surface of the host fruit over irregular intervals throughout the female's life. Approximately 100 eggs are laid by a single female over her life time. However under ideal temperatures, the number of eggs laid by a single female may reach 800 eggs. Egg hatching rate is temperature dependent, where by higher temperatures correlate with an increase in egg maturity rate. The period from oviposition to hatching may range from 9-14 days with hatching occurring at any time of the day [39]. A newly hatched larvae are creamy-white with a black head. The hatched larvae burrow into the fruit of the host

plant through a hole that they create on the fruit. This results in a discoloration of fruit around the burrowed area. Once the larvae are inside the fruit they begin to feed on the fruit. As they get older, they move towards the centre of the fruit. This causes the fruit to ripen and drop before the harvest season and also makes the damaged fruit to become undesirable, vulnerable and prone to secondary pests such as fungal organisms, bacteria, scavengers . A mature larvae is approximately 10-15mm in length and pink-red in color . The mature larvae then exit the fruit through frass filled exit holes where they then drop to the ground on silken threads [39].

In the pupal stage, the FCM larvae spin a white-cream colored cocoon in the soil before they emerge as adults. The length of this stage is both temperature and gender dependent whereby warmer periods are correlated with a more rapid rate of emergence, and cooler temperatures reduce the process to a slower rate. Pupae are cream colored and soft at first but then harden and darken as they mature. Pupae are sensitive to cold temperatures and rainfall when young The pupae emerge out of the cocoon just before the adult emerges out of the pupal casing [30]. Pupation and emergence of adults occurs in the spring and is temperature-dependent [10]. Adult FCM are small and inconspicuous. They are inactive during the day, where they take refuge in shaded portions of the host plant, and are only active during portions of the night. The male lifespan is between 14 and 57 days, whereas females may live between 16 and 70 days. Adults have patterned wings of 12.5 to 20 mm in a variation of colors, including grey, brown, black, and orange-brown. To attract males, adult females release pheromone at night, a few hours after dark, peaking at five hours and then decreasing thereafter until sunrise [10].

[12] conducted a study on area- wide control tactics for the false codling moth by integrating the sterile release technique with the release of the egg parasitoid. In the study, both treated males and females were released into the field together with the parasitoid *Trichogramma cryptophlebia*. The result showed that the combined field release of the irradiated false codling moth and the parasitoid resulted in a rapid increase in the population of the parasitoid, which had a positive impact on the suppression of the false codling moth population, which is more effective than when either technique was employed separately. False codling moth is a phytosanitary pest and impedes export on most international markets, as it is endemic in sub-Saharan Africa [20, 28]. Consequently, the intercept of even an individual pest in a consignment could lead to the rejection of the entire consignment [28, 27]. [8] also conducted a study on the radiation biology and inherited sterility of false codling moth. They examined the effect of increasing doses of gamma irradiation on the fecundity and fertility of false codling moth. Newly emerged adults as well as mature pupae were treated with doses of radiation and adults were in-bred to fertility counter parts. the results from their study showed that fecundity was not adversely affected by dose of radiation when untreated females were mated to treated females. However, the fecundity of treated females mated to either untreated or treated males declined as the dose of radiation increased.

[31] studied the effects of fecundity, mortality and distribution of the initial condition in phenological model based on a system of partial differential equations. The temporal

dynamics of a stage-structured population and the distribution of the individuals on physiological age within each stage was also established. In the study fecundity dependent on physiological age and on temperature. The study reported that the introduction of the fecundity as a function of the adult physiological age and temperature can change the dynamics depending on the oviposition profile with respect to the physiological age. They recommended that fecundity, mortality and age distribution should always be considered for the purpose of model definition and calibration in pest management for proper decision in the implementation of pest control strategies.

[16] developed a computational mathematical model to study the movement and stag-specific habitat preferences of a polyphagous insects. In the study, they reported that parent-offspring conflict always emerge as providing the best host for offspring development is detrimental to adult survival and fecundity. The parent-offspring conflict was simulated when adult insects exploit two crops (Corn and Soybean) which provide different nutritional advantages for each insect stage. The study reported that there exist an optimal period of time in which insect alternate between each host.

Chemical pesticides have been widely used to control pest populations such as FCM for a long time in the world [23]. However, its widespread use has resulted in environmental pollution and a reduction in natural pest enemies, resulting in unfavourable environmental side effects [11]. Furthermore, the emergence of insect resistance to chemical products has increased the demand for stronger and more toxic pesticides in order to maintain efficacy. Therefore, the widespread use of pesticides is not a long-term pest-control solution [2]. As a result, there is growing interest in the development of non-polluting control strategies; these strategies place a special emphasis on the ecology and behaviour of the involved species [5]. Therefore, to prevent devastating impacts on the economy, and ensure adequate food security, social life, health, and biodiversity; efficient control, understanding of biodiversity, and management of FCM are essential [2, 40]. One of the most promising strategies is the use of Pheromone trap [22] and sterile insect technique (SIT).

Mathematical modeling is a method of simulating real-life situations with mathematical equations to predict future behavior by generating a simplified representation of a real system [1, 33]. Mathematical modeling is an important tool that can be used in studying biological and agricultural phenomena. The application of mathematical theory to the problem allows a qualitative and quantitative evaluation of the cases of interest (Adul Latif, 2014). A mathematical model describes a system by a set of state variables and equations that establish relationships between those variables and the governing parameters [34, 21]. These models are useful experimental tools for building and testing theories, assessing quantitative conjectures, answering specific questions, determining sensitivities to changes in parameter values, and estimating key parameters from data [22, 33].

Mathematical models can also be used in comparing, predicting, planning, implementing, evaluating, and optimizing various detection, prevention, therapy, and control programs [21, 22]. The models can further help in getting better understanding of the dynamics of the pest population, and various control strategies can be studied to optimise the

control of pest population [3, 2]. Mathematical models are built on biological and ecological knowledge of the population dynamics, independently from specific observation data. Although, the output of mathematical models is not as good in fitting observation data, they are less costly, more flexible and offer the possibility to change the settings and simulate various scenarios [34, 1, 16].

This paper, seeks to develop a mathematical model of the sterile insect technique for control of FCM. This will shed more light on the control strategies of the insect pest population.

2. Preliminaries

Articles should be divided into sections and subsections. Principal sections should be written consecutively, e.g., as

3. Model Formulation

The proposed model for the sterile insect techniques for control of FCM, is a modified version of [22]. The model is subdivided into nine compartments representing the susceptible host population (S), the FCM egg population (E), the FCM larval population (L), the FCM pupal population (P), the mature female (F), the mature male population (M), the fertilized female population (F_f), the non-fertilized female population (F_n) and the sterile male population (M_s). Following successful mating with the fertile male, the fertile female lays fertile eggs on the susceptible host, which hatch into larvae that burrow into the fruit. We assume that the susceptible fruit's growth rate follows a logistic growth model, and that once the larvae attack the susceptible fruit, it is removed. The sterile insects are introduced into the FCM's wild population. When a fertile female FCM mates with a sterile male FCM, the fertile female lays eggs that do not hatch into larvae. A set of differential equations that describe the transfer of individuals between classes is used to model the host FCM interaction.

The susceptible host is harvested at rate μ and the environmental carrying capacity of susceptible host is K_h with α as the intrinsic growth rate of the susceptible host. Assume that larval attacks rate is ξ , m is the half-saturation constant. It is important to note that, at the larval stage, FCM is most destructive to the susceptible host. The sterile insect directly affects the fertile male female compartment, Assume that fertile eggs are laid only by fertilised fertile females after a successful mating with fertile males at time t and r is the intrinsic egg laying rate, A is the carrying capacity of the fertile egg at the susceptible host, ϕ is the egg conversion rate, λ_1 is the transfer rate from the fertile egg stage to the fertile larva, and ω_1 is the natural egg mortality rate. The larval conversion rate is given by α and the transfer rate from the larval stage to the pupal stage are λ_2 and ω_2 is the natural larval mortality rate. λ_3 is the number of fertile pupa that move to the adult stage and ω_3 is the mortality rate of the pupal stage.

After emergence from the pupal stage, the FCM can be a fertile female or a fertile male, κ is the fraction of the pupal population that emerged in fertile female. After laying

egg the fertilised fertile female that returned to fertile female at rate δ_1 , δ_2 represents the fraction of non fertilised fertile female that returned to fertile female after mating with the sterile insect and after laying non-hatching eggs, λ_4 is the transfer rate of fertile female fertilised fertile female or non-fertilised fertile female, and ω_4 is the natural mortality rate of fertile female. The fraction of the pupal population that goes to the fertile male compartment is given by $(1 - \kappa)$. where ω_5 is the natural mortality of the fertile male. If the sterile insect is released at a rate of ψ and q is the fraction of the sterile male released that joins the wild FCM population and ω_8 is the natural mortality of the sterile insect, and μ is the mating competitiveness of the sterile male. If the fraction of fertile females that mate with the fertile male and move to the fertilised fertile female compartment to lay a fertile egg is given by q_1 , then q_2 represents the fraction of fertile females that mate with the sterile male and move to the non-fertilised fertile female compartment and lay non-hatching eggs, with ω_6 representing the natural mortality of fertilised female and ω_7 is the natural mortality of non-fertilised fertile female. The system of ordinary differential equations which describe the interaction of susceptible host, FCM and sterile insect is as follows:

$$\begin{aligned}
\frac{dS(t)}{dt} &= \alpha \left(1 - \frac{S(t)}{K_h} \right) S(t) - \frac{\xi S(t)L(t)}{m + S(t)} - \mu_1 S(t) \\
\frac{dE(t)}{dt} &= rF_f(t) \left(1 - \frac{E(t)}{A} \right) \phi S(t) - (\lambda_1 + \omega_1)E(t) \\
\frac{dL(t)}{dt} &= \lambda_1 E(t) + \frac{\alpha \xi S(t)L(t)}{m + S(t)} - (\lambda_2 + \omega_2)L(t) \\
\frac{dP(t)}{dt} &= \lambda_2 L(t) - (\lambda_3 + \omega_3)P(t) \\
\frac{dF(t)}{dt} &= \kappa \lambda_3 P(t) + \delta_1 F_f(t) + \delta_2 F_n(t) - q_1 M(t)F(t) - q_2 M_s(t)F(t) - \omega_4 F(t) \\
\frac{dM(t)}{dt} &= (1 - \kappa) \lambda_3 P(t) - \omega_5 M(t) \\
\frac{dF_f(t)}{dt} &= q_1 M(t)F(t) - (\delta_1 + \omega_6(t)) F_f(t) \\
\frac{dF_n(t)}{dt} &= q_2 M_s(t)F(t) - (\delta_2 + \omega_7(t)) F_n(t) \\
\frac{dM_s(t)}{dt} &= \psi q \mu - \omega_8 M_s(t)
\end{aligned} \tag{3.1}$$

Where $S(t) \geq 0, E(t) \geq 0, L(t) \geq 0, P(t) \geq 0, F(t) \geq 0, M(t) \geq 0, F_f(t) \geq 0, F_n(t) \geq 0, M_s(t) \geq 0$

3.1. Model Analysis

To preserve the biological validity of the model, the solutions to the system of differential equations 11 must be positive and finite for all time values. Declaring a population as negative, for example, is not biologically feasible. Additionally, populations must be finite in number, since both plants and pests have a finite number of cells. Furthermore, boundedness and positivity demonstrate that once FCM attacks a susceptible host, its population can persist below the detectable threshold [41]. To make the solution of system 1

model mathematically and entomologically meaningful, it must demonstrate that its state variables are positive and bounded for all time t . That is, the system solution with a positive initial value will remain positive for all time $t \geq 0$. This can be demonstrated using Theorem 1:

Theorem 3.1. *If the initial conditions of the model system 1 are in domain \mathcal{D} such that:*

$$\mathcal{D} = \{(S(t), E(t), L(t), P(t), F(t), M(t), F_f(t), F_n(t), M_s(t)) \\ \in \mathfrak{R}_+^9 : N(t) \leq \frac{\hat{k}}{q} (\alpha + 1) + \varepsilon\}$$

Then all solutions of system equation 1 enter and remain in the same domain \mathcal{D} :

Proof. Consider the set $S(t), E(t), L(t), P(t), F(t), M(t), F_f(t), F_n(t), M_s(t)$ with any solution of system model 1 such that the total population is expressed as $N(t) = S(t) + E(t) + L(t) + P(t) + F(t) + M(t) + F_f(t) + F_n(t) + M_s(t)$ and $\frac{dN(t)}{dt} = \frac{dS}{dt} + \frac{dE}{dt} + \frac{dL}{dt} + \frac{dP}{dt} + \frac{dF}{dt} + \frac{dM}{dt} + \frac{dF_f}{dt} + \frac{dF_n}{dt} + \frac{dM_s}{dt}$. Now, using the foregoing expression in the addition of system model 1, yields:

$$\frac{dN(t)}{dt} = \frac{d}{dt} \{S(t) + E(t) + L(t) + P(t) + F(t) + M(t) + F_f(t) + F_n(t) + M_s(t)\} \quad (3.2)$$

$$\begin{aligned} \frac{dN(t)}{dt} &= \frac{dS}{dt} + \frac{dE}{dt} + \frac{dL}{dt} + \frac{dP}{dt} + \frac{dF}{dt} + \frac{dM}{dt} \\ &\quad + \frac{dF_n}{dt} + \frac{dM_s}{dt} + \frac{dF_p}{dt} \\ &\quad + \left[\alpha \left(1 - \frac{S(t)}{K_h} \right) S(t) - \frac{\xi S(t)L(t)}{m + S(t)} - \mu_1 S(t) \right] \\ &\quad + \left[r F_f(t) \left(1 - \frac{E(t)}{A} \right) \phi S(t) - (\lambda_1 + \omega_1) E(t) \right] \\ &\quad + \left[\lambda_1 E(t) + \frac{\alpha \xi S(t)L(t)}{m + S(t)} - (\lambda_2 + \omega_2) L(t) \right] \\ &\quad + [\lambda_2 L(t) - (\lambda_3 + \omega_3) P(t)] \\ &\quad + [\kappa \lambda_3 P(t) + \delta_1 F_f(t) + \delta_2 F_n(t) - q_1 M(t) F(t) - q_2 M_s(t) F(t) - \omega_4 F(t)] \\ &\quad + [(1 - \kappa) \lambda_3 P(t) - \omega_5 M(t)] M(t) \\ &\quad + [q_1 M(t) F(t) - (\delta_1 + \omega_6(t)) F_f(t)] \\ &\quad + [q_2 M_s(t) F(t) - (\delta_2 + \omega_7(t)) F_n(t)] \\ &\quad + [\psi q \mu - \omega_8 M_s(t)] \end{aligned}$$

This simplifies to:

where $\hat{k} = \max\{S(0), K\}$ and $\Psi = \min\{1, \omega_1, \omega_2, \omega_3, \omega_4, \omega_5, \omega_6, \omega_7 + \tau_8 \omega_8\}$ Then

$$\frac{dN}{dt} + \Psi N = \hat{k}(\alpha + 1)$$

and its solutions become

$$N(t) \leq \frac{\hat{k}}{\Psi}(\alpha + 1)(1 - \exp(-\Psi t)) + N(0) \exp(-\Psi t)$$

At $t \rightarrow \infty$, we have $N(t) \leq \frac{\hat{k}}{\Psi}(\alpha + 1)$. Implies that the solution is bounded for $0 \leq N \leq \frac{\hat{k}}{\Psi}(\alpha + 1)$. Thus, all solutions of the model system 1 in \mathfrak{R}_+^9 are restricted in the region: $\mathcal{D} = \{(S(t), E(t), L(t), P(t), F(t), M(t), F_f(t), F_n(t), M_s(t)) \in \mathfrak{R}_+^9 : N(t) \leq \frac{\hat{k}}{q}(\alpha + 1) + \varepsilon\}$ for all $\varepsilon > 0$ and $t \rightarrow 0$. The models system 11's solutions reveal the time evolution of individuals within each class. The solution must correspond to natural phenomena for any dynamic system to be well-posed [7]. As a result, it is established that the feasible solution set for the host-pest interaction model is positively invariant, biologically meaningful, and mathematically well posed. \square

3.2. Equilibria Analysis

From a biological perspective, the equilibria points are classified into three main equilibria points of interest: FCM free equilibrium points (E_0), SIT free equilibrium points (E_1), combined co-existence equilibrium points (E_2).

3.2.1. FCM free equilibrium points (E_0)

At the FCM-free equilibrium points (E_0), it is assumed that there is no pest prevalence in the system; hence the population of the susceptible host grows logistically to maturity. It is further assumed that there is no need for control methods. Therefore, to analyse the equilibrium points without FCM in system model 1, the FCM components and control components are set to zero, such that: $E^* = 0, L^* = 0, P^* = 0, F^* = 0, M^* = 0, F_f^* = 0, F_n^* = 0, M_s^* = 0$. This is achieved by setting the right-hand sides of the 1 equations of the host-pest interaction model to zero, given by: $E_0 = (S^*, E^*, L^*, P^*, F^*, M^*, F_f^*, F_n^*, M_s^*)$. If ($E^* = 0, L^* = 0, P^* = 0, F^* = 0, M^* = 0, F_f^* = 0, F_n^* = 0, M_s^* = 0$), then the equations representing the pest compartment reduce to zero to yield:

$$E_0 = (K_h(\alpha - \mu_1), 0, 0, 0, 0, 0, 0, 0, 0) \quad (3.3)$$

3.2.2. SIT free equilibrium points (E_1)

At SIT free equilibrium points (E_2), the false codling moths freely interacts with the host without the presence of sterile insects in the population, it is a steady state solution where FCM coexist naturally in the susceptible host population in the absence of sterile insect males in the population. Therefore, the compartments of the sterile insect technique of model system 11 are set to zero, such that $E_2 = (S^{o\&}, E^{o\&}, L^{o\&}, P^{o\&}, F^{o\&}, M^{o\&}, F_f^{o\&})$, and solve for the values of $S^{o\&}, E^{o\&}, L^{o\&}, P^{o\&}, F^{o\&}, M^{o\&}, F_f^{o\&}$ as shown in Equation 4:

$$\begin{aligned}
0 &= \alpha \left(1 - \frac{S(t)}{K_h}\right) S(t) - \frac{\xi S(t)L(t)}{m + S(t)} - \mu_1 S(t) \\
0 &= rF_f(t) \left(1 - \frac{E(t)}{A}\right) \phi S(t) - (\lambda_1 + \omega_1)E(t) \\
0 &= \lambda_1 E(t) + \frac{\alpha \xi S(t)L(t)}{m + S(t)} - (\lambda_2 + \omega_2)L(t) \\
0 &= \lambda_2 L(t) - (\lambda_3 + \omega_3)P(t) \\
0 &= \kappa \lambda_3 P(t) + \delta_1 F_f(t) + \delta_2 F_n(t) - q_1 M(t)F(t) - q_2 M_s(t)F(t) - \omega_4 F(t) \\
0 &= (1 - \kappa)\lambda_3 P(t) - \omega_5 M(t) \\
0 &= \lambda_4 q_1 M(t)F(t) - (\delta_1 + \omega_6(t)) F_f(t) \\
0 &= q_2 M_s(t)F(t) - (\delta_2 + \omega_7(t)) F_n(t) \\
0 &= \psi q \mu - \omega_8 M_s(t)
\end{aligned} \tag{3.4}$$

Solving equation 4, yields 5:

$$\begin{aligned}
S^{o\&}(t) &= -\frac{1}{2} \left[\left(\mu_1 + \frac{m}{K_h} - \alpha \right) K_h \pm \sqrt{\left(\mu_1 + \frac{m}{K_h} - \alpha \right)^2 - 4(\xi L^{o\&} + \mu m - \alpha m)K_h} \right] \\
E^{o\&}(t) &= \frac{ArF_f^{o\&}(t)S^{o\&}(t)}{rF_f^{*o\&}(t)S^{o\&}(t) + A(\lambda_1 + \omega_1)} \\
L^{o\&} &= \frac{\lambda_1 E^{o\&}}{(\lambda_2 + \omega_2) \left((\lambda_2 + \omega_2) - \frac{\alpha \xi S^{o\&}}{m + S^{o\&}} \right)} \\
P^{o\&} &= \frac{\lambda_2 L^{o\&}}{(\lambda_3 + \omega_3)} \\
F^{o\&} &= \frac{\kappa \lambda_3 P^{o\&} + \delta_1 F_f^{o\&}}{\omega_4 + \lambda_4} \\
M^{o\&} &= \frac{(1 - \kappa)\lambda_3 P^{o\&}}{\omega_5} \\
F_f^{o\&} &= \frac{M^{o\&} F_f^{o\&}}{(\delta_1 + \omega_6)}
\end{aligned} \tag{3.5}$$

The equation 5 can be solved numerically using MATLAB software based on the values of the parameters in Table 1. The solutions are graphically illustrated in Figures 1 and 2. Figure 1 illustrates the dynamic of the total FCM population with time at the control free equilibrium. From figure 1, it is observed that the total population of FCM rises sharply from the initial population to maximum, then drops to below 400 and then starts to rise again and stabilises at about 900 total population size of FCM where the control free equilibrium exists.

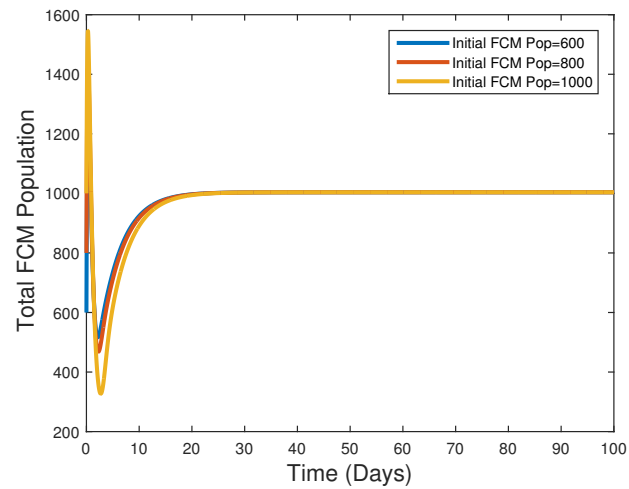


Figure 1: Total FCM Population Against Time Without Control

Figure 2 illustrates the dynamic of the susceptible host population over time at the free control equilibrium. In Figure 2, it can be shown that the equilibrium point is reached at a value lower than the carrying capacity of the susceptible host ($K_h = 1000$). These results from Figures 1 and 2 show the effect of FCM infestation on the susceptible host population when there is no control measure.

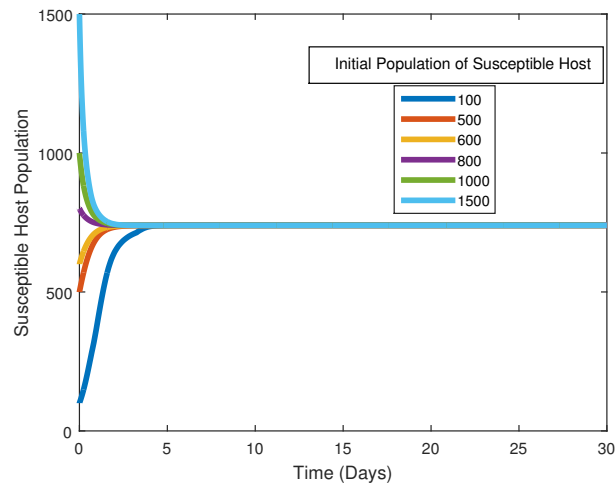


Figure 2: Susceptible Host Population against Time without Control

3.2.3. co-existence equilibrium points (E_2)

At Co-existence equilibrium points, the sterile insect, the FCM and the host naturally coexists, such that, $E_3 = (S^{**\&, E^{**\&, L^{**\&, P^{**\&, F^{**\&, M^{**\&, F_f^{**\&, F_n^{**\&, M_s^{**\&}$). The co-existence equilibrium point is the steady-state solution in which FCM co-exists naturally in a population of susceptible hosts with only a sterile insect as a control agent. To achieve this, the equations on the right-hand side of the host host-FCM interaction model 11 equations is equated to zero as shown in Equation 18, and for the values of $S^{**\&, E^{**\&, L^{**\&, P^{**\&, F^{**\&, M^{**\&, F_f^{**\&, F_n^{**\&, M_s^{**\&}$.

$$\begin{aligned}
0 &= \alpha \left(1 - \frac{S^{**\&(t)}}{K_h} \right) S^{**\&(t)} - \frac{\xi S^{**\&(t)} L^{**\&(t)}}{m + S^{**\&(t)}} - \mu_1 S^{**\&(t)} \\
0 &= r F_f^{**\&(t)} \left(1 - \frac{E^{**\&(t)}}{A} \right) \phi S^{**\&(t)} - (\lambda_1 + \omega_1) E^{**\&(t)} \\
0 &= \lambda_1 E^{**\&(t)} + \frac{\alpha \xi S^{**\&(t)} L^{**\&(t)}}{m + S^{**\&(t)}} - (\lambda_2 + \tau_2 \omega_2) L^{**\&(t)} \\
0 &= \lambda_2 L^{**\&(t)} - (\lambda_3 + \omega_3) P^{**\&(t)} \\
0 &= \kappa \lambda_3 P^{**\&(t)} + \delta_1 F_f^{**\&(t)} + \delta_2 F_n^{**\&(t)} - \left[\lambda_4 \left(\frac{M^{**\&(t)}}{M^{**\&(t)} + M_s^{**\&(t)}} \right) + \omega_4 \right] F^{**\&(t)} \\
0 &= (1 - \kappa) \lambda_3 P^{**\&(t)} - \omega_5 M^{**\&(t)} \\
0 &= \lambda_4 \left(\frac{M^{**\&(t)}}{M^{**\&(t)} + M_s^{**\&(t)}} \right) F_f^{**\&(t)} - (\delta_1 + \omega_6(t)) F_f^{**\&(t)} \\
0 &= \lambda_4 \left(\frac{\mu M_s^{**\&(t)}}{M^{**\&(t)} + M_s^{**\&(t)}} \right) F_n^{**\&(t)} - (\delta_2 + \omega_7(t)) F_n^{**\&(t)} \\
0 &= \psi q \mu - \omega_8 M_s^{**\&(t)}
\end{aligned} \tag{3.6}$$

Solving equation system 6, yields equation 7 and 8:

$$\begin{aligned}
S^{**\&(t)} &= -\frac{1}{2} \left[\left(\mu_1 + \frac{m}{K_h} - \alpha \right) K_h \pm \sqrt{\left(\mu_1 + \frac{m}{K_h} - \alpha \right)^2 - 4(\xi L^{**\& + \mu m - \alpha m) K_h} \right] \\
E^{**\&(t)} &= \frac{A r \phi F_f^{**\&(t)} S^{**\&(t)}}{r \phi F_f^{**\&(t)} S^{**\&(t)} + A(\lambda_1 + \omega_1)} \\
L^{**\& &= \frac{\lambda_1 E^{**\&}}{(\lambda_2 + \omega_2) \left((\lambda_2 + \omega_2) - \frac{\alpha \xi S^{**\&}}{m + S^{**\&}} \right)} \\
P^{**\& &= \frac{\lambda_2 L^{**\&}}{(\lambda_3 + \omega_3)}
\end{aligned} \tag{3.7}$$

$$\begin{aligned}
F^{**\&} &= \frac{\kappa\lambda_3 P^{**\&}}{\omega_4 - \frac{\delta_2\lambda_4}{(\delta_2 + \omega_7)(M^{**\&} \frac{\omega_8}{\psi q \mu} + 1)} + \frac{\omega_6\lambda_4 M^{**\&}}{(\delta_1 + \omega_6)(M^{**\&} + \frac{\psi q \mu}{\tau_8 \omega_8})}} \\
M^{**\&} &= \frac{\frac{\lambda_4 + \omega_4 - \delta_1}{\kappa\lambda_3}}{\omega_5} \\
F_f^{**\&} &= \frac{\lambda_4 M^{**\&} F_f^{**\&}}{(\delta_1 + \omega_6)(M^{**\&} + \frac{\psi q \mu}{\omega_8})} \\
F_n^{**\&} &= \frac{\lambda_4}{(\delta_2 + \omega_7)(M^{**\&} \frac{\omega_8}{\psi q \mu} + 1)} F_f^{**\&} \\
M_s^{**\&} &= \frac{\psi q \mu}{\omega_8}
\end{aligned} \tag{3.8}$$

Equations 7 and 8 are solved using MATLAB software based on the parameters outlined in Table 1. The numerical solution is represented graphically in Figure 4. Figure 3 depicts the total pest population versus time at the pheromone traps free equilibrium points under different FCM initial populations. From figure 3, the total population of FCM first increases from the initial population to maximum, then drops gradually and level off at the equilibrium point. The increase of FCM population at first is because the number of sterile insects released had not reached the optimal level in order to offer control, but after the threshold value of pheromone is released is reached, the population of FCM starts to decrease gradually. It converges at the equilibrium point irrespective of the initial population of the FCM.

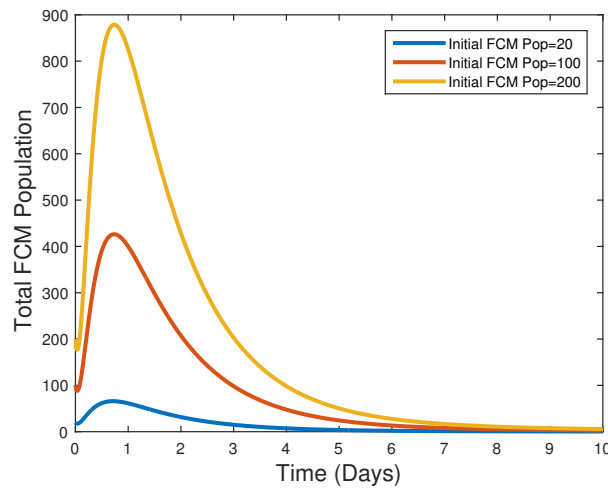


Figure 3: Total Population of FCM Against Time in the Presence of SIT

3.3. Basic Reproduction Number

In epidemiological models, the next-generation matrix has been extensively used to calculate basic reproduction numbers. However, its application in entomology is limited, and many entomological models do not use the next-generation matrix approach to determine the basic reproduction number of a system of ordinary differential equations [17]. However, [17] used the next-generation matrix method to investigate the autonomy and stability of the predator-prey model. [17] defined "basic reproduction number" as the number of offspring produced by a mature predator during its lifetime when introduced in a prey-only environment with prey at carrying capacity. Other studies, such as [3] and [3] have also used the next generation matrix to find the basic reproduction number of entomological systems.

In this study, we follow the method outlined by [22], which yields equation 9:

$$\mathcal{R}_0 = \frac{\alpha K_h(\alpha - \mu_1)\xi}{(m + K_h(\alpha - \mu_1))(\lambda_2 + \omega_2)} \quad (3.9)$$

The basic reproduction number measures the mean number of new offspring produced by fertilised fertile females in an entirely susceptible host population with carrying capacity without control. Since the basic reproduction number is less than unity, the likelihood of FCM infestation in the susceptible host will be lower under control; that is, when the sterile insects technique is used as control measures of FCM. However, changes in parameter values that affect the basic reproduction number can increase basic reproduction, leading to a FCM outbreak if proper mitigation is not used.

3.4. Stability Analysis

When studying dynamical systems, determining the long-term behaviour of a system and locating crucial points that define the system's stability both need knowledge of the idea of linear stability, which is why this specific aspect of the study of dynamical systems is so vitally significant. In control theory, it is utilised to build controllers that stabilise unstable systems. Additionally, it is used in engineering and physics to investigate the stability of structures and fluid flows [1].

3.4.1. Local Stability Analysis

Local stability of the equilibrium points of model system 1 is investigated in order to establish whether if there is a small perturbation of the system (for example, a small number of false codling moths is introduced into the population), then after some time the system will return to the equilibrium point. Local stability analysis is performed by constructing the Jacobian matrix of model system 11 and solving it at the equilibrium points: FCM free equilibrium point, control free equilibrium point, and co-existence equilibrium points. Now, let system 11 be written in vector form as given in Equation 10:

$$\frac{dy}{dt} = f(x) \quad (3.10)$$

where:

$$x = (S(t), E(t), L(t), P(t), F(t), M(t), F_f(t), F_n(t), M_s(t))$$

Then, the function x can be written in matrix form as shown in Equation 11:

$$f(x) = \begin{pmatrix} \alpha \left(1 - \frac{S(t)}{K_h}\right) S(t) - \frac{\xi S(t)L(t)}{m+S(t)} - \mu_1 S(t) \\ rF_f(t) \left(1 - \frac{E(t)}{A}\right) \phi S(t) - (\lambda_1 + \omega_1)E(t) \\ \lambda_1 E(t) + \frac{a\xi S(t)L(t)}{m+S(t)} - (\lambda_2 + \omega_2)L(t) \\ \lambda_2 L(t) - (\lambda_3 + \omega_3)P(t) \\ \kappa\lambda_3 P(t) + \delta_1 F_f(t) + \delta_2 F_n(t) - \left[\lambda_4 \left(\frac{M(t)}{M(t)+\mu M_s(t)}\right) + \omega_4\right] F(t) \\ (1 - \kappa)\lambda_3 P(t) - [\omega_5] M(t) \\ \lambda_4 \left(\frac{M(t)}{M(t)+\mu M_s(t)}\right) F_f(t) - (\delta_1 + \omega_6(t)) F_f(t) \\ \lambda_4 \left(\frac{\mu M_s(t)}{M(t)+\mu M_s(t)}\right) F_f(t) - (\delta_2 + \omega_7(t)) F_n(t) \\ \psi q \mu - [\omega_8] M_s(t) \end{pmatrix} \quad (3.11)$$

The right-hand side of Equation 11 is a continuous local Lipschitz function, so the uniqueness and local existence of the solution are guaranteed. By computing the Jacobian matrix of Equation 11, we obtain Equation 12:

$$J_f = \begin{pmatrix} x_1 & 0 & x_2 & 0 & 0 & 0 & 0 & 0 & 0 & 0 \\ x_3 & x_4 & 0 & 0 & 0 & 0 & x_5 & 0 & 0 & 0 \\ x_6 & x_7 & x_8 & 0 & 0 & 0 & 0 & 0 & 0 & 0 \\ 0 & 0 & x_9 & x_{10} & 0 & 0 & 0 & 0 & 0 & 0 \\ 0 & 0 & 0 & x_{11} & x_{12} & x_{13} & x_{14} & x_{15} & x_{16} & 0 \\ 0 & 0 & 0 & x_{17} & x_{18} & x_{19} & 0 & 0 & 0 & 0 \\ 0 & 0 & 0 & 0 & x_{21} & x_{22} & x_{23} & 0 & x_{24} & 0 \\ 0 & 0 & 0 & 0 & x_{25} & x_{26} & 0 & x_{27} & x_{28} & 0 \\ 0 & 0 & 0 & 0 & 0 & 0 & 0 & 0 & 0 & x_{30} \end{pmatrix} \quad (3.12)$$

Where: $x_1 = \alpha - \frac{2S}{K_h} - \frac{\xi L(m+S) - \xi SL}{(m+S)^2} - \mu_1$, $x_2 = -\frac{\xi S}{m+S}$, $x_3 = r\phi F_f \left(1 - \frac{E}{A}\right)$, $x_4 = -\frac{r\phi F_f S}{A} - (\lambda_1 + \omega_2)$, $x_5 = rS$, $x_6 = \frac{a\xi L}{(m+S)^2}$, $x_7 = \lambda_1$, $x_8 = \frac{a\xi S}{m+S} - (\lambda_2 + \omega_2)$, $x_9 = \lambda_2$, $x_{10} = -(\lambda_3 + \omega_3)$, $x_{11} = \kappa\lambda_3$, $x_{12} = -\frac{\lambda_4 M}{M+M_s} - \omega_4$, $x_{13} = \frac{\mu M_s}{M+\mu M_s}$, $x_{14} = \delta_1$, $x_{15} = \delta_2$, $x_{16} = -\lambda_4 \frac{M}{(M+M_s)^2} F$, $x_{17} = (1 - \kappa)\lambda_3$, $x_{18} = 0$, $x_{19} = -[\omega_5]$, $x_{20} = 0$, $x_{21} = \lambda_4 \left(\frac{M}{M+\mu M_s}\right)$, $x_{22} = \lambda_4 \left(\frac{\mu M_s}{(M+\mu M_s)^2}\right) F$, $x_{23} = -(\delta_1 + \omega_6)$, $x_{24} = \lambda_4 \left(\frac{\mu M}{(M+\mu M_s)^2}\right) F$, $x_{25} = \lambda_4 \left(\frac{\mu M}{(M+\mu M_s)^2}\right)$, $x_{26} = -\lambda_4 \left(\frac{\mu M}{(M+\mu M_s)^2}\right) F$, $x_{27} = -(\delta_2 + \omega_7)$, $x_{28} = \frac{\mu(M+\mu M_s) - \mu M_s}{(M+\mu M_s)^2}$, $x_{30} = -\omega_8$.

The Jacobian matrix 12 was subjected to an equilibrium analysis.

3.4.2. Local Stability Analysis of FCM free Equilibrium Points

Theorem 3.2. *The free equilibrium point of FCM E_0 is locally asymptotically stable if $R_0 < 1$ and otherwise unstable.*

Proof. The local stability analysis of model system 1 can be determined by solving the Jacobian matrix 12 at the free equilibrium points of FCM ($E_0 = (K_h(\alpha - \mu_1), 0, 0, 0, 0, 0, 0, 0, 0, 0)$), which yields Equation 13:

$$\mathcal{J}_f|_{E_0} = \begin{pmatrix} x_1 & 0 & x_2 & 0 & 0 & 0 & 0 & 0 & 0 \\ 0 & x_4 & 0 & 0 & 0 & 0 & x_5 & 0 & 0 \\ 0 & x_7 & x_8 & 0 & 0 & 0 & 0 & 0 & 0 \\ 0 & 0 & x_9 & x_{10} & 0 & 0 & 0 & 0 & 0 \\ 0 & 0 & 0 & x_{11} & x_{12} & x_{13} & x_{14} & x_{15} & 0 \\ 0 & 0 & 0 & x_{17} & 0 & x_{19} & 0 & 0 & 0 \\ 0 & 0 & 0 & 0 & 0 & 0 & x_{23} & 0 & 0 \\ 0 & 0 & 0 & 0 & x_{25} & 0 & 0 & 0 & 0 \\ 0 & 0 & 0 & 0 & x_{29} & 0 & 0 & 0 & 0 \end{pmatrix} \quad (3.13)$$

Where: $x_1 = \mu_1 - \alpha$, $x_2 = -\frac{\xi K_h(\alpha - \mu_1)}{m + K_h(\alpha - \mu_1)} = -R_0 \frac{(\lambda_2 + \omega_2)}{a}$, $x_4 = -(\lambda_1 + \omega_1)$, $x_5 = rK_h(\alpha - \mu_1)$, $x_7 = \lambda_1$, $x_8 = \frac{a\xi K_h(\alpha - \mu_1)}{m + K_h(\alpha - \mu_1)} - (\lambda_2 + \omega_2) = \frac{(\lambda_2 + \omega_2)(R_0 - a)}{a}$, $x_9 = \lambda_2$, $x_{10} = -(\lambda_3 + \omega_3)$, $x_{11} = \kappa\lambda_3$, $x_{12} = -\omega_4$, $x_{13} = \frac{1}{\mu(\frac{\psi q \mu}{\omega_8})}$, $x_{14} = \delta_1$, $x_{15} = \delta_2$, $x_{17} = (1 - \kappa)\lambda_3$, $x_{19} = -[\omega_5]$, $x_{23} = -(\delta_1 + \omega_6)$, $x_{25} = \lambda_4$, $x_{27} = -0$, $x_{28} = 0$, $x_{29} = 0$, $x_{30} = 0$.

Matrix 13 is solved using the Wolfram Mathematica software, which yields the eigenvalues shown in Equation 14:

$$\begin{aligned} s_1 &= 0 \\ s_3 &= -\alpha + \mu_1 \\ s_4 &= -\lambda_1 - \omega_1 \\ s_5 &= \frac{-a\lambda_2 + R_0\lambda_2 - a\omega_2 + R_0\omega_2}{a} \\ s_6 &= -\lambda_3 - \omega_3 \\ s_7 &= \frac{1}{2} \left(-\omega_4 - \sqrt{4\delta_2\lambda_4 + \omega_4^2} \right) \\ s_8 &= \frac{1}{2} \left(-\omega_4 - \sqrt{4\delta_2\lambda_4 + \omega_4^2} \right) \\ s_9 &= -\omega_5 \\ s_{10} &= -\delta_1 - \omega_6 \end{aligned} \quad (3.14)$$

The stability of the free equilibrium point of FCM E_0 is determined by the values of s_5 and s_3 . Since $\alpha > \mu_1$, the value of s_3 remains negative. Therefore, the stability of E_0 is determined by s_5 , which simplifies to equation 15:

$$s_5 = \frac{(\lambda_2 + \omega_2)(R_0 - a)}{a} \quad (3.15)$$

From Equation 15, the values of the parameters λ_2 , ω_2 , and a remain positive. As a result, the stability of the FCM-free equilibrium is determined by the value of the larval conversion efficiency $0 < a \leq 1$ such that if $R_0 < a$, then s_5 becomes negative and the FCM-free equilibrium is said to be asymptotically stable, otherwise unstable if $R_0 > a$. This implies that if the population of the susceptible host is small, the conversion efficiency will also be minimal. Therefore, the growth and survival of FCM depend on the availability of the susceptible host. \square

3.4.3. Local Stability Analysis of SIT free Equilibrium Points

The local stability analysis of model system 11 can be established by solving the Jacobian matrix 12 at the free control equilibrium points (E_2), which yields Equation 16:

$$J_f|_{E_2} = \begin{pmatrix} x_1 & 0 & x_2 & 0 & 0 & 0 & 0 & 0 & 0 \\ x_3 & x_4 & 0 & 0 & 0 & 0 & x_5 & 0 & 0 \\ x_6 & x_7 & x_8 & 0 & 0 & 0 & 0 & 0 & 0 \\ 0 & 0 & x_9 & x_{10} & 0 & 0 & 0 & 0 & 0 \\ 0 & 0 & 0 & x_{11} & x_{12} & 0 & x_{14} & x_{15} & x_{16} \\ 0 & 0 & 0 & x_{17} & 0 & x_{19} & 0 & 0 & 0 \\ 0 & 0 & 0 & 0 & x_{21} & 0 & x_{23} & 0 & x_{24} \\ 0 & 0 & 0 & 0 & x_{25} & x_{26} & 0 & x_{27} & x_{28} \\ 0 & 0 & 0 & 0 & x_{29} & 0 & 0 & 0 & x_{30} \end{pmatrix} \quad (3.16)$$

Where: $x_1 = \alpha - \frac{2S^{*\&}}{K_h} - \frac{\xi L^{*\&}(m+S^{*\&}) - \xi S^{*\&L^{*\&}}{(m+S^{*\&})^2} - \mu_1$, $x_2 = -\frac{\xi S^{*\&}}{m+S^{*\&}}$, $x_3 = r\phi F_f^{*\&} \left(1 - \frac{E^{*\&}}{A}\right)$, $x_4 = -\frac{r\phi F_f^{*\&}S^{*\&}}{A} - (\lambda_1 + \omega_2)$, $x_5 = rS^{*\&}$, $x_6 = \frac{a\xi L^{*\&}}{(m+S^{*\&})^2}$, $x_7 = \lambda_1$, $x_8 = \frac{a\xi S^{*\&}}{m+S^{*\&}} - (\lambda_2 + \omega_2)$, $x_9 = \lambda_2$, $x_{10} = -(\lambda_3 + \omega_3)$, $x_{11} = \kappa\lambda_3$, $x_{12} = -\lambda_4 - \omega_4$, $x_{13} = 0$, $x_{14} = 0$, $x_{15} = \delta_2$, $x_{16} = -\lambda_4 \frac{1}{M^{*\&}} F^{*\&}$, $x_{17} = (1 - \kappa)\lambda_3$, $x_{18} = 0$, $x_{19} = \omega_5$, $x_{20} = 0$, $x_{21} = \lambda_4$, $x_{22} = 0$, $x_{23} = -\omega_6$, $x_{24} = \lambda_4 \left(\frac{1}{M^{*\&}}\right) F^{*\&}$, $x_{25} = \lambda_4$, $x_{26} = -\lambda_4 \left(\frac{1}{M^{*\&}}\right) F^{*\&}$, $x_{27} = -\omega_7$, $x_{28} = \frac{1}{M^{*\&}}$, $x_{30} = -(\omega_8)$. With the values of $S^{*\&}$, $E^{*\&}$, $L^{*\&}$, $P^{*\&}$, $F^{*\&}$, $M^{*\&}$, $F_f^{*\&}$. Matrix 36 is solved using Wolfram Mathematica software, which produces the eigenvalues as: $s_1 = x_{19}$, $s_2 = s_3 = s_4 = s_5 = s_6 = x_{10}x_{14}x_2x_{21}x_4x_6 - x_{10}x_{12}x_2x_{23}x_4x_6 - x_1x_{10}x_{14}x_{12}x_4x_8 + x_1x_{10}x_{12}x_{23}x_4x_8 + (x_1x_{10} + x_1x_{12} + x_{10}x_{12} - x_{14}x_{21} + x_1x_{23} + x_{10}x_{23} + x_{12}x_{23} + x_1x_4 + x_{10}x_4 + x_{12}x_4 + x_{23}x_4 - x_2x_6 + x_1x_8 + x_{10}x_8 + x_{12}x_8 + x_{23}x_8 + x_4x_8) + (-x_1 - x_{10} - x_{12} - x_{23} - x_4 - x_8)$. Through back-substitution, all the eigenvalues are found to be negative. Therefore, the control-free equilibrium point is a stable equilibrium point. System 1 is said to be locally asymptotically stable around the control equilibrium points E_2 .

3.4.4. Local Stability Analysis of Coexistence Equilibrium Points

The local stability analysis of model system 11 can be established by solving the Jacobian matrix 20 at the co-existence equilibrium point, which yields equation 17:

$$J_3 = \begin{pmatrix} x_1 & 0 & x_2 & 0 & 0 & 0 & 0 & 0 & 0 \\ x_3 & x_4 & 0 & 0 & 0 & 0 & x_5 & 0 & 0 \\ x_6 & x_7 & x_8 & 0 & 0 & 0 & 0 & 0 & 0 \\ 0 & 0 & x_9 & x_{10} & 0 & 0 & 0 & 0 & 0 \\ 0 & 0 & 0 & x_{11} & x_{12} & x_{13} & x_{14} & x_{15} & x_{16} \\ 0 & 0 & 0 & x_{17} & 0 & x_{19} & 0 & 0 & 0 \\ 0 & 0 & 0 & 0 & x_{21} & x_{22} & x_{23} & 0 & x_{24} \\ 0 & 0 & 0 & 0 & x_{25} & x_{26} & 0 & x_{27} & x_{28} \\ 0 & 0 & 0 & 0 & x_{29} & 0 & 0 & 0 & x_{30} \end{pmatrix} \quad (3.17)$$

Where: $x_1 = \alpha - \frac{2S^{**\&}}{K_h} - \frac{\xi L^{**\&}(m+S^{**\&}) - \xi S^{**\&L^{**\&}}{(m+S^{**\&})^2} - \mu_1$, $x_2 = -\frac{\xi S^{**\&}}{m+S^{**\&}}$, $x_3 = rF_f^{**\&} \left(1 - \frac{E^{**\&}}{A}\right)$, $x_4 = -\frac{r\phi F_f^{**\&}S^{**\&}}{A} - (\lambda_1 + \omega_2)$, $x_5 = r\phi S^{**\&}$, $x_6 = \frac{a\xi L^{**\&}}{(m+S^{**\&})^2}$, $x_7 = \lambda_1$, $x_8 = \frac{a\xi S^{**\&}}{m+S^{**\&}} -$

$(\lambda_2 + \omega_2)$, $x_9 = \lambda_2$, $x_{10} = -(\lambda_3 + \omega_3)$, $x_{11} = \kappa\lambda_3$, $x_{12} = -\frac{\lambda_4 M^{**\&}}{M^{**\&} + M_s^{**\&}} - \omega_4$, $x_{13} = \frac{\mu M_s^{**\&}}{M^{**\&} + \mu M_s^{**\&}}$, $x_{14} = \delta_1$, $x_{15} = \delta_2$, $x_{16} = -\lambda_4 \frac{M^{**\&}}{(M^{**\&} + M_s^{**\&})^2} F^{**\&}$, $x_{17} = (1 - \kappa)\lambda_3$, $x_{19} = -\omega_5$, $x_{20} = -\left(\frac{1}{(F^{**\&})}\right) M^{**\&}$, $x_{21} = \lambda_4 \left(\frac{M^{**\&}}{M^{**\&} + \mu M_s^{**\&}}\right)$, $x_{22} = \lambda_4 \left(\frac{\mu M_s^{**\&}}{(M^{**\&} + \mu M_s^{**\&})^2}\right) F^{**\&}$, $x_{23} = -(\delta_1 + \omega_6)$, $x_{24} = \lambda_4 \left(\frac{\mu M_s^{**\&}}{(M^{**\&} + \mu M_s^{**\&})^2}\right) F^{**\&}$, $x_{25} = \lambda_4 \left(\frac{\mu M_s^{**\&}}{(M^{**\&} + \mu M_s^{**\&})^2}\right)$, $x_{26} = -\lambda_4 \left(\frac{\mu M_s^{**\&}}{(M^{**\&} + \mu M_s^{**\&})^2}\right) F^{**\&}$, $x_{27} = -(\delta_2 + \omega_7)$, $x_{28} = \frac{\mu(M^{**\&} + \mu M_s^{**\&}) - \mu M_s^{**\&}}{(M^{**\&} + \mu M_s^{**\&})^2}$, $x_{30} = -\omega_8$,
 With the values of $S^{**\&}$, $E^{**\&}$, $L^{**\&}$, $P^{**\&}$, $F^{**\&}$, $M^{**\&}$, $F_f^{**\&}$, $F_n^{**\&}$, $M_s^{**\&}$ are given in Equation 16. The eigenvalues of matrix 17 in (E_3) are found to be: $s_1 = [-y_{10}y_{16}y_{19}y_{23}y_{27}y_{29}y_{4}y_6 + y_{10}y_{14}y_{19}y_{23}y_{27}y_{29}y_{4}y_6 + (-y_1 - y_{10} - y_{12} - y_{19} - y_{23} - y_{27} - y_{30}y_4 - y_8)]$,
 $s_2 = s_3 = [-y_{10}y_{16} \dots y_4y_6]$, $s_4 = s_5 = s_6 = s_7 = s_8 = s_9 = [y_{10}y_{16}y_{19}y_{23}y_{27}y_{29}y_{4}y_6 + y_{10}y_{14}y_{19}y_{23}y_{27}y_{29}y_{4}y_6 + y_{10}y_{14}y_{19}y_{23}y_{27}y_{29}y_{4}y_6]$. Through back substitution, all eigenvalues of the coexistence equilibrium point are found to be negative, which shows that E_3 is a stable equilibrium point. Therefore, system 1 is locally asymptotically stable around the free equilibrium point of the sterile insect technique E_3 .

This implies that when the sterile insect technique is used as a control measure for FCM, a stable equilibrium point is achieved, provided that all parameters affecting the basic reproduction number are not affected. However, any change in the parameter value in Model System 1 may lead to an unstable point in the system that otherwise would be unstable.

3.5. Global Stability Analysis

Global stability analysis is performed using the Metzler matrix stability method proposed by [13] and the Lyapunov method.

3.5.1. Global Stability Analysis of E_0

Assuming the system is cooperative on \mathbb{R}_+^9 , growth in any compartment has a positive impact on growth in all other compartments. The global stability of the equilibrium without FCM is investigated using the Metzler matrix stability method proposed by [13].

The method of [13] is where system model 11 is written as shown in Equation 18:

$$\begin{aligned}
 \frac{dX}{dt} &= F(X, Z) \\
 \frac{dZ}{dt} &= G(X, Z), G(X, 0) = 0
 \end{aligned} \tag{3.18}$$

Where: $X = (S, M_s) \in \mathbb{R}_+^2$ denotes non-infectious compartments and $Z = (E, L, P, F, M, F_f, F_n) \in \mathbb{R}_+^7$ denotes infectious pest compartments. $E_0 = (X^*, 0)$ represents the pest free equilibrium of the system. If this point satisfies the following conditions: (i) for $\frac{dX}{dt} = F(X, 0)$, where X^* is globally asymptotically stable, (ii) $\frac{dZ}{dt} = D_z G(X, 0)Z - G(X, Z)$, $G(X, Z) \geq 0$ for all $(X, Z) \in \Omega$, then we can conclude that E_0 is globally asymptotically stable if The following Theorem 3 holds:

Theorem 3.3. *The equilibrium point $E_0 = (X^*, 0)$ of system 18 is globally asymptotically stable if conditions (i) and (ii) are satisfied, otherwise unstable.*

Proof. Let $X = (S, M_s)$ and $Z = (E, L, P, F, M, F_f, F_n)$ be the new variables and the subsystems of the system model 1. From Equation 28, two vector-valued functions $G(X, Z)$ and $F(X, Z)$ can be given by Equations 19 and 20:

$$F(X, Z) = \begin{pmatrix} \alpha \left(1 - \frac{S(t)}{K_h}\right) S(t) - \frac{\xi S(t)L(t)}{m+S(t)} - \mu_1 S(t) \\ \psi q \mu - \omega_8 M_s(t) \end{pmatrix} \quad (3.19)$$

and

$$G(X, Z) = \begin{pmatrix} rF_f(t) \left(1 - \frac{E(t)}{A}\right) \phi S(t) - (\lambda_1 + \tau_1 \omega_1) E(t) \\ \lambda_1 E(t) + \frac{\alpha \xi S(t)L(t)}{m+S(t)} - (\lambda_2 + \omega_2) L(t) \\ \lambda_2 L(t) - (\lambda_3 + \omega_3) P(t) \\ \kappa \lambda_3 P(t) + \delta_1 F_f(t) + \delta_2 F_n(t) - \left[\lambda_4 \left(\frac{M(t)}{M(t) + \mu M_s(t)} \right) + \omega_4 \right] F(t) \\ (1 - \kappa) \lambda_3 P(t) - \omega_5 M(t) \\ \lambda_4 \left(\frac{M(t)}{M(t) + \mu M_s(t)} \right) F_f(t) - (\delta_1 + \omega_6(t)) F_f(t) \\ \lambda_4 \left(\frac{\mu M_s(t)}{M(t) + \mu M_s(t)} \right) F_f(t) - (\delta_2 + \omega_7(t)) F_n(t) \end{pmatrix} \quad (3.20)$$

Now, let us consider the reduced system, $\frac{dX}{dt} = F(X, 0)$ from condition (i) yields equation 21:

$$\begin{aligned} \frac{dS}{dt} &= \alpha \left(1 - \frac{S(t)}{K_h}\right) S(t) - \mu S(t) \\ \frac{dM_s}{dt} &= \psi q \mu - \omega_8 M_s(t) \end{aligned} \quad (3.21)$$

It is observed that this is an asymptomatic dynamics system, independent of the initial conditions in Ω ; therefore, the convergence of the solutions of the reduced system 18 is global in Ω . By computing:

$$G(X, Z) = D_z G(X^*, 0) - \hat{G}(X, Z)$$

and showing that

$$\hat{G}(X, Z) \geq 0$$

Now, let $B = D_z G(X^*, 0)$, which is the Jacobian of $\hat{G}(X, Z)$ taken in $(E, L, P, F, M, F_f, F_n)$ and evaluated at $(X^*, 0)$. Then the matrix B is given by Equation 22:

$$B = \begin{pmatrix} x_1 & 0 & 0 & 0 & 0 & x_2 & 0 \\ x_3 & x_4 & 0 & 0 & 0 & 0 & 0 \\ 0 & x_5 & x_6 & 0 & 0 & 0 & 0 \\ 0 & 0 & x_7 & x_8 & 0 & x_9 & x_{10} \\ 0 & 0 & x_{11} & 0 & x_{12} & 0 & 0 \\ 0 & 0 & 0 & 0 & 0 & x_{13} & 0 \\ 0 & 0 & 0 & x_{14} & 0 & 0 & x_{15} \end{pmatrix} \quad (3.22)$$

Where: $x_1 = -(\lambda_1 + \omega_1)$, $x_2 = -rK_h(\alpha - \mu_1)$, $x_3 = \lambda_1$, $x_4 = \frac{\alpha \xi K_h(\alpha - \mu_1)}{m + K_h(\alpha - \mu_1)} - (\lambda_2 + \omega_2)$, $x_5 = \lambda_2$, $x_6 = -(\lambda_3 + \omega_3)$, $x_7 = \kappa \lambda_3$, $x_8 = -\omega_4$, $x_9 = \delta_1$, $x_{10} = \delta_2$, $x_{11} = (1 - \kappa) \lambda_3$, $x_{12} = -\omega_5$, $x_{13} = -(\delta_1 + \omega_6)$, $x_{14} = \lambda_4$, $x_{15} = -(\delta_2 + \omega_7)$.

The value of $\hat{G}(X, Z)$ is given by Equation 23:

$$\hat{G}(X, Z) = \begin{pmatrix} r\phi F_f(t) \left(1 - \frac{E(t)}{A}\right) (K_h(\alpha - \mu_1) - S(t)) \\ a\xi L(t) \left(\frac{K_h(\alpha - \mu_1)}{m + (K_h(\alpha - \mu_1))} - \frac{S}{m + S}\right) \\ 0 \\ 0 \\ 0 \\ 0 \\ 0 \end{pmatrix} \quad (3.23)$$

Since $K_h \geq S$. It is clear that $\hat{G}(X, Z) \geq 0$ for all $(X, Z) \in \mathcal{D}$, then the pest-free equilibrium will be globally asymptotically stable. It is also important to note that matrix B is an M -matrix since all off-diagonal elements are nonnegative. Therefore, this proves that PFE is globally asymptotically stable. \square

These results imply that the FCM-free equilibrium will be globally asymptotically stable. However, whenever the FCM dynamics population changes, the free FCM equilibrium may not be globally asymptotically stable.

3.5.2. Global Stability Analysis of E_1

The global stability of control free equilibrium points is performed using the Lyapunov method of stability analysis. By constructing a suitable Lyapunov function, an approach adopted by [24] is used. Consider the Lyapunov function in Equation 24:

$$L = \sum a_i (y_i - x_i^{o\&} \ln y_i) \quad (3.24)$$

Where a_i is the constant selected such that $a_i > 0$, y_i is the population of the compartment i th and $y_i^{o\&}$ is the free equilibrium point of control. Therefore, expanding the Lyapunov function in Equation 24 in model system 1 at control-free equilibrium points yields Equation 25:

$$L = a_1(S - S^{o\&} \ln S) + a_2(E - E^{o\&} \ln E) + a_3(L - L^{o\&} \ln L) + a_4(P - P^{o\&} \ln P) \\ + a_5(F - F^{o\&} \ln F) + a_6(M - M^{o\&} \ln M) + a_7(F_f - F_f^{o\&} \ln F_f) \quad (3.25)$$

Differentiating 24 with respect to time yields equation 26:

$$\begin{aligned}
 \frac{dL}{dt} = & a_1 \left(1 - \frac{S^{o\&}}{S}\right) \frac{dS}{dt} + a_2 \left(1 - \frac{E^{o\&}}{E}\right) \frac{dE}{dt} + a_3 \left(1 - \frac{L^{o\&}}{L}\right) \frac{dL}{dt} + a_4 \left(1 - \frac{P^{o\&}}{P}\right) \frac{dP}{dt} \\
 & + a_5 \left(1 - \frac{F^{o\&}}{F}\right) \frac{dF}{dt} + a_6 \left(1 - \frac{M^{o\&}}{M}\right) \frac{dM}{dt} + a_7 \left(1 - \frac{F_f^{o\&}}{F_f}\right) \frac{dF_f}{dt} \\
 = & a_1 \left(1 - \frac{S^{o\&}}{S}\right) \left[\alpha \left(1 - \frac{S(t)}{K_h}\right) S(t) - \frac{\xi S(t)L(t)}{m + S(t)} - \mu_1 S(t) \right] \\
 & + a_2 \left(1 - \frac{E^{o\&}}{E}\right) \left[r F_f(t) \left(1 - \frac{E(t)}{A}\right) S(t) - (\lambda_1 + \tau_1 \omega_1) E(t) \right] \\
 & + a_3 \left(1 - \frac{L^{o\&}}{L}\right) \left[\lambda_1 E(t) + \frac{\alpha \xi S(t)L(t)}{m + S(t)} - (\lambda_2 + \tau_2 \omega_2) L(t) \right] \\
 & + a_4 \left(1 - \frac{P^{o\&}}{P}\right) [\lambda_2 L(t) - (\lambda_3 + \tau_3 \omega_3) P(t)] \\
 & + a_5 \left(1 - \frac{F^{o\&}}{F}\right) [\kappa \lambda_3 P(t) + \delta_1 F_f(t) - (\lambda_4 + \tau_4 \omega_4) F(t)] \\
 & + a_6 \left(1 - \frac{M^{o\&}}{M}\right) [(1 - \kappa) \lambda_3 P(t) - \tau_5 \omega_5 M(t)] \\
 & + a_7 \left(1 - \frac{F_f^{o\&}}{F_f}\right) [\lambda_4 F_f(t) - (\delta_1 + \tau_6 \omega_6(t)) F_f(t)]
 \end{aligned} \tag{3.26}$$

Where: $S(t) = S^{o\&}$, $E(t) = E^{o\&}$, $L(t) = L^{o\&}$, $P(t) = P^{o\&}$, $F(t) = F^{o\&}$, $M(t) = M^{o\&}$, $F_f(t) = F_f^{o\&}$.

Following [26] approach, and assuming that system model 1 is positively invariant, equation 26 is non-positive. Hence $\frac{dL}{dt} \leq 0 \forall S, E, L$, $P, F, M, F_f > 0$ and is zero when $S(t) = S^{o\&}$, $E(t) = E^{o\&}$, $L(t) = L^{o\&}$, $P(t) = P^{o\&}$, $F(t) = F^{o\&}$, $M(t) = M^{o\&}$, $F_f(t) = F_f^{o\&}$. Therefore, the largest invariant set in $\{(S^{o\&}, E^{o\&}, L^{o\&}, P^{o\&}, F^{o\&}, M^{o\&}, F_f^{o\&}) \in \mathcal{D}\}$ such that $\frac{dL}{dt} = 0$ is the singleton $\{E_2\}$ which is the control free equilibrium point. According to the invariant principle put forward by [25], E_2 is globally asymptotically stable in \mathcal{D} , if $R_0 \geq 1$ the interior of \mathcal{D} , otherwise unstable.

An important question by entomologists is whether, pest, after a possible outbreak, will persist and stay and stay in a positive infestation level over time, and whether this behaviour depends on the initial size of the pest. Mathematically, this is represented by the global asymptotic stability of the control free equilibrium.

3.5.3. Global Stability Analysis of E_2

Theorem 3.4. *The sufficient condition for global stability of the model system 1 is that the coexistence equilibrium point is feasible and has a locally asymptomatic stable solution.*

Proof. Global stability of coexistence equilibrium points is constructed using a suitable

Lyapunov function, an approach adopted by [24]. In this approach, the Lyapunov function is constructed based on equation 27:

$$L = \sum a_i (x_i - x_i^{**\&} \ln x_i) \quad (3.27)$$

Where a_i is the constant selected such that $a_i > 0$, x_i is the population of the i th compartment and $x_i^{**\&}$ is the equilibrium point of co-existence. Therefore, consider the Lyapunov function in Equation 28:

$$\begin{aligned} L = & a_1(S - S^{**\&} \ln S) + a_2(E - E^{**\&} \ln E) + a_3(L - L^{**\&} \ln L) + a_4(P - P^{**\&} \ln P) \\ & + a_5(F - F^{**\&} \ln F) + a_6(M - M^{**\&} \ln M) + a_7(F_f - F_f^{**\&} \ln F_f) \\ & + a_8(F_n - F_n^{**\&} \ln F_n) + a_9(M_s - M_s^{**\&} \ln M_s) \end{aligned} \quad (3.28)$$

Differentiating 28 with respect to time yields equation 29:

$$\begin{aligned} \frac{dL}{dt} = & a_1 \left(1 - \frac{S^{**\&}}{S} \right) \frac{dS}{dt} + a_2 \left(1 - \frac{E^{**\&}}{E} \right) \frac{dE}{dt} + a_3 \left(1 - \frac{L^{**\&}}{L} \right) \frac{dL}{dt} + a_4 \left(1 - \frac{P^{**\&}}{P} \right) \frac{dP}{dt} \\ & + a_5 \left(1 - \frac{F^{**\&}}{F} \right) \frac{dF}{dt} + a_6 \left(1 - \frac{M^{**\&}}{M} \right) \frac{dM}{dt} + a_7 \left(1 - \frac{F_f^{**\&}}{F_f} \right) \frac{dF_f}{dt} \\ & + a_8 \left(1 - \frac{F_n^{**\&}}{F_n} \right) \frac{dF_n}{dt} + a_9 \left(1 - \frac{M_s^{**\&}}{M_s} \right) \frac{dM_s}{dt} \\ = & a_1 \left(1 - \frac{S^{**\&}}{S} \right) \left[\alpha \left(1 - \frac{S(t)}{K_h} \right) S(t) - \frac{\xi S(t)L(t)}{m + S(t)} - \mu_1 S(t) \right] \\ & + a_2 \left(1 - \frac{E^{**\&}}{E} \right) \left[r\phi F_f(t) \left(1 - \frac{E(t)}{A} \right) S(t) - (\lambda_1 + \omega_1)E(t) \right] \\ & + a_3 \left(1 - \frac{L^{**\&}}{L} \right) \left[\lambda_1 E(t) + \frac{\alpha \xi S(t)L(t)}{m + S(t)} - (\lambda_2 + \omega_2)L(t) \right] \\ & + a_4 \left(1 - \frac{P^{**\&}}{P} \right) [\lambda_2 L(t) - (\lambda_3 + \omega_3)P(t)] \\ & + a_5 \left(1 - \frac{F^{**\&}}{F} \right) \left[\kappa \lambda_3 P(t) + \delta_1 F_f(t) + \delta_2 F_n(t) - \left[\lambda_4 \left(\frac{M(t)}{M(t) + M_s(t)} \right) + \tau_4 \omega_4 \right] F(t) \right] \\ & + a_6 \left(1 - \frac{M^{**\&}}{M} \right) [(1 - \kappa) \lambda_3 P(t) - \omega_5] M(t) \\ & + a_7 \left(1 - \frac{F_f^{**\&}}{F_f} \right) \left[\lambda_4 \left(\frac{M(t)}{M(t) + M_s(t)} \right) F_f(t) - (\delta_1 + \omega_6(t)) F_f(t) \right] \\ & + a_8 \left(1 - \frac{F_n^{**\&}}{F_n} \right) \left[\lambda_4 \left(\frac{M_s(t)}{M(t) + M_s(t)} \right) F_f(t) - (\delta_2 + \omega_7(t)) F_n(t) \right] \\ & + a_9 \left(1 - \frac{M_s^{**\&}}{M_s} \right) \end{aligned} \quad (3.29)$$

Where: $S(t) = S^{**\&}$, $E(t) = E^{**\&}$, $L(t) = L^{**\&}$, $P(t) = P^{**\&}$, $F(t) = F^{**\&}$, $M(t) = M^{**\&}$, $F_f(t) = F_f^{**\&}$, $F_n(t) = F_n^{**\&}$, $M_s(t) = M_s^{**\&}$.

Following the approach of [26], it can easily be seen that equation 29 is non-positive. Hence $\frac{dL}{dt} \leq 0 \forall S, E, L, P, F, M, F_f, F_n, M_s, F_p > 0$ and is zero when $S(t) = S^{**}, E(t) = E^{**}, L(t) = L^{**}, P(t) = P^{**}, F(t) = F^{**}, M(t) = M^{**}, F_f(t) = F_f^{**}, F_n(t) = F_n^{**}, M_s(t) = M_s^{**}$. Therefore, the largest invariant set in $\{(S^{**}, E^{**}, L^{**}, P^{**}, F^{**}, M^{**}, F_f^{**}, F_n^{**}, M_s^{**}) \in \mathcal{D}\}$ such that $\frac{dL}{dt} = 0$ is the singleton $\{E_3\}$ which is the the pheromone traps free equilibrium point. According to the invariant principle put forward by [25], E_3 is globally asymptotically stable in \mathcal{D} , if $R_0 \leq 1$ the interior of \mathcal{D} , otherwise unstable. According to [25] invariant principle, E_3 is globally asymptotically stable in \mathcal{D} if $R_0 \leq 1$ is the interior of \mathcal{D} , otherwise unstable. \square

These results imply that the pheromone trap free equilibrium will be globally asymptotically stable whenever the basic reproduction number is less than unity. However, whenever the FCM dynamics population changes and the sterile release rate changes, the pheromone trap free equilibrium may not be globally asymptotically stable.

The FCM infestation may occur at the least time expected if the FCM was feeding on other host plants, which may lead to the random distribution of FCM throughout the host population, a linear relationship between host harvesting and FCM burden may occur. Thus, for a given pattern of FCM distribution, a particular functional response may stabilise the dynamics, whereas others may result in instabilities, as in the case of predator-prey association. As a result, it is worthwhile to conduct a bifurcation analysis to determine the system's global stability further.

4. Sensitivity Analysis of the Model

Sensitivity analysis is performed to identify key parameters that can significantly impact the dynamics of the host-FCM interaction model. To determine which key parameters to consider in the control FCM population. The initial FCM population is directly related to R_0 , and the coexistence of host and FCM is directly related to the equilibria points. To investigate the potential impact of pheromone traps and sterile insect techniques on the population of FCM, sensitivity analysis of the basic reproduction number with respect to pheromone traps and sterile insect technique is carried out.

Sensitivity analysis indices of the basic reproduction number R_0 and the coexistence equilibrium point E_5 to the parameter in the model system 4.1.1 are performed following the method of [7] and [13].

Definition 4.1. The normalized forward-sensitivity index of a variable \mathcal{R}_0 , that depends differentially on parameter, μ_i is defined as in equation 30:

$$\gamma_{\mu_i}^{\mathcal{R}_0} = \frac{\partial \mathcal{R}_0}{\partial \mu_i} \times \frac{\mu_i}{\mathcal{R}_0} \quad (4.1)$$

Where μ_i represents all the main parameters and

$$\mathcal{R}_0 = \frac{\alpha \xi K_h (\alpha - \mu_1)}{(m + K_h (\alpha - \mu_1)) (\lambda_2 + \omega_2)}$$

From the definition, the parameters of the basic reproduction number, which are affected by pheromone concentration and sterile insect technique, are ξ , α , λ_2 , and ω_2 , since they have a direct link to the FCM dynamics. Changes in pheromone concentration and sterile insect release rate directly affect the magnitude of these parameters. Therefore, the sensitivity of the pheromone trap and sterile insect release rate with respect to the basic reproduction number is analysed based on these parameters. To find the sensitivity index of the harvesting term (ξ) we proceed as shown in equation 31:

$$\begin{aligned} \gamma_{\xi}^{\mathcal{R}_0} &= \frac{\partial \mathcal{R}_0}{\partial \xi} \times \frac{\xi}{\mathcal{R}_0} \\ &= \frac{\alpha \xi K_h (\alpha - \mu_1)}{(m + K_h (\alpha - \mu_1)) (\lambda_2 + \omega_2)} \frac{\xi}{\frac{\alpha \xi K_h (\alpha - \mu_1)}{(m + K_h (\alpha - \mu_1)) (\lambda_2 + \omega_2)}} \\ &= 1 > 0 \end{aligned} \quad (4.2)$$

Since the sensitivity index of ξ is positive, its increase increases the basic reproduction number, leading to more FCM infestation. Therefore, to decrease the value of this parameter, the value of pheromone concentration and sterile release rate should be increased. A plot of the FCM attack rate (ξ) against the basic reproduction number is illustrated in Figure 4. From Figure 4, it is seen that an increase in conversion rate leads to a corresponding increase in the basic reproduction number.

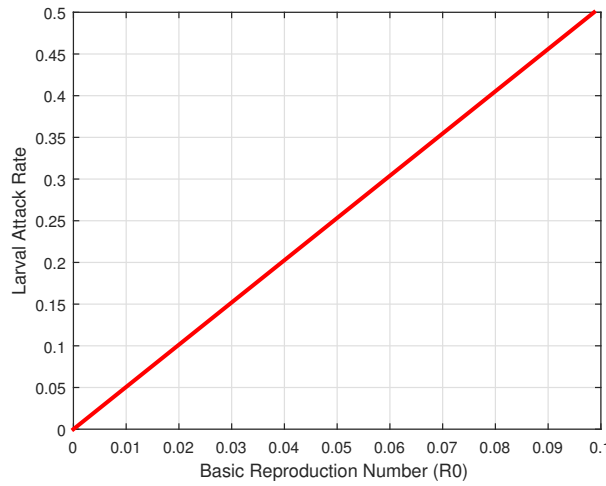


Figure 4: Attack Rate against Basic Reproduction Number \mathcal{R}_0

To find the sensitivity index of conversion rate (α) we proceed as shown in equation

32:

$$\begin{aligned}
\Upsilon_a^{\mathcal{R}_0} &= \frac{\partial \mathcal{R}_0}{\partial a} \times \frac{a}{\mathcal{R}_0} \\
&= \frac{\xi K_h(\alpha - \mu_1)}{(m + K_h(\alpha - \mu_1))(\lambda_2 + \omega_2)} \times \frac{a}{\frac{a \xi K_h(\alpha - \mu_1)}{(m + K_h(\alpha - \mu_1))(\lambda_2 + \omega_2)}} \\
&= 1.0 > 0
\end{aligned} \tag{4.3}$$

Since the sensitivity index of a is positive, its increase leads also to increase in the basic reproduction number which further leads to more FCM infestation. A plot of FCM conversion rate against the basic reproduction number is illustrated in Figure 5. From the Figure its observed that an increase in conversion rate lead to a corresponding increase in the basic reproduction number.

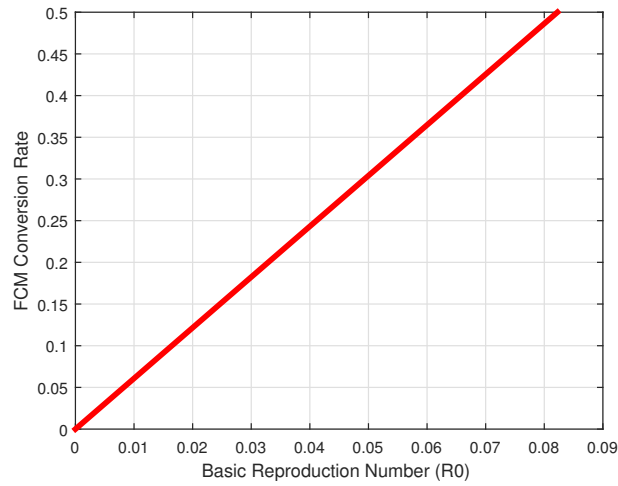


Figure 5: FCM Conversion Rate against Basic Reproduction Number \mathcal{R}_0

A similar procedure can be used to calculate the sensitivity indices of other parameters around the basic reproduction number, is summarised in Table 2:

Table 1: Sign of Sensitivity Index

Parameter	Sensitivity Index	Value
α	Positive	0.0001921737
μ_1	Negative	-0.0000043
a	Positive	1.0
ξ	Positive	1.0
K_h	Positive	0.000189
m	Negative	-0.0003786
λ_2	Negative	-0.066217
ω_2	Negative	-0.96

4.1. Interpretation of Sensitivity Indices

The sensitivity indices of the basic reproduction number R_0 with respect to the main parameters are illustrated in Table 5. Parameters with positive indices (K_h, α, ξ) have a greater impact on FCM infestation in the susceptible host population, since the increase in their values increases \mathcal{R} , in the model system 1. On the other hand, parameters whose sensitivity index is negative ($m, \mu_1, \lambda_2, \omega_2$) have the effect of minimising the burden of FCM infestation in the susceptible host population. As their values increase, the basic reproduction number decreases, which minimises the pest burden in the susceptible host population. In this study, pheromone traps and sterile insect techniques can minimise the values of parameters whose sensitivity indices are positive. Therefore, with sensitivity analysis, you can obtain information on the appropriate intervention strategies to prevent and control the spread of the pest in the population.

4.2. Numerical Simulations

Numerical simulations of the 1 model system are carried out to illustrate some of the analytical results of the study system and to understand the effect of the sterile insect technique and pheromone traps on the population of susceptible FCM hosts. A set of reasonable parameter values was used as given in Table 1. These parameter values were obtained from the literature and some of them were assumed following reasonable ecological observations. In this study, $S(t) = 100, E(t) = 0, L(t) = 0, P(t) = 0, F(0) = 20, M(0) = 20, F_f(0) = 0, F_n = 0, M_s = 0$, were considered as the initial values for the simulation of the model system 1 with a time range between 0 and 100 days, in addition to the parameter values in Table 1. Numerical simulations of the effect of FCM on the susceptible host without control and the impact of the sterile insect technique on the FCM and susceptible host populations are carried out $0 \leq t \leq 100$ in days in Matlab software and presented in graphical form.

4.2.1. Effect of the Absence of FCM on Susceptible Host

The effect of FCM on the susceptible host can be analysed by first evaluating the growth pattern of the susceptible host in the absence of the false codling moth, then introducing FCM on the farm and evaluating the growth pattern of the susceptible host in the presence of FCM. In the absence of FCM, the susceptible host population grows logistically and levels off at carrying capacity. The absence of FCM in the host population can be numerically illustrated by setting the FCM compartments and the sterile insect compartment in model system 1 to zero and using the other remaining parameters as indicated in Table 1.

Figure 6 shows a graph of susceptible host and FCM populations against time when there is no harvest on the farm such that $\mu_1 = 0.0$. The figure shows that the susceptible host population increases logistically to its carrying capacity ($K_h = 1000$) while the FCM population remains zero throughout. This shows that in the absence of FCM, the farmer will achieve high crop yields. Therefore, to improve crop production, an attempt must be made to ensure that the false codling moth is eliminated on the farm.

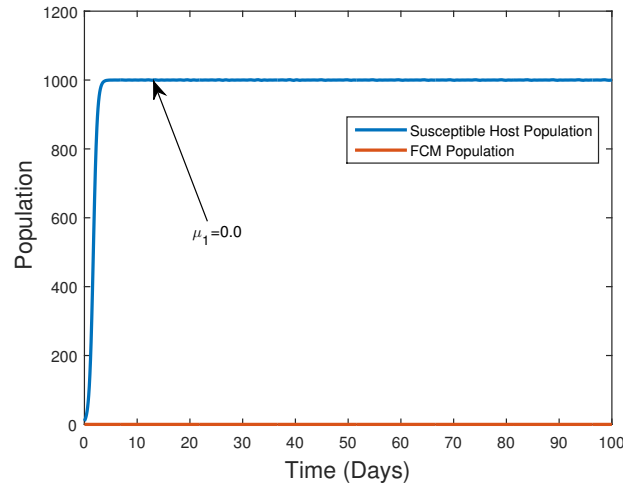


Figure 6: A plot of susceptible host and FCM populations in time with $\mu_1 = 0.0$

In this study, the harvesting term represents other ways susceptible hosts can be removed, other than through FCM inversion. When the harvest term is extended to such that $\mu_1 = 0.2$, the susceptible host population continues to grow logistically, but does not reach the host's carrying capacity, while the FCM population remains constant throughout, as illustrated in Figure 7. Therefore, when μ_1 increases, susceptible hosts do not reach their carrying capacity.

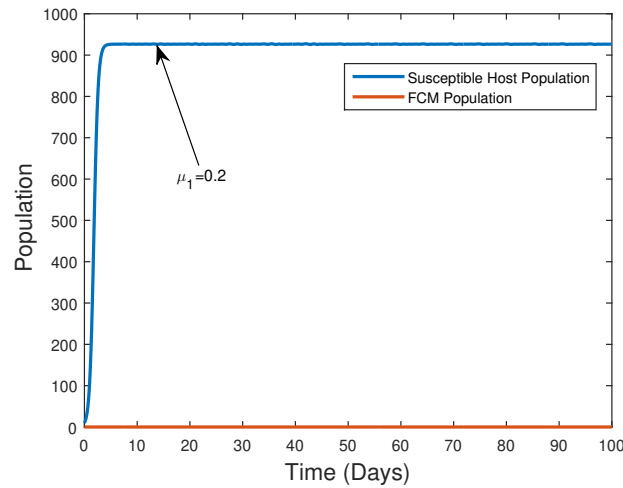


Figure 7: A Graph of the Susceptible Host against Time with $\mu_1 = 0.2$

Therefore, in the absence of FCM in the field with zero harvesting term, farmers would realise maximum crop yields. Therefore, it is necessary to completely eliminate FCM on the farm.

4.2.2. The Impact of FCM on the Host

The effect of FCM on the susceptible host is determined by performing numerical simulations of the host-pest interaction model with the parameters in the sterile insect compartment set to zero, that is, $\psi = 0$, $\omega_8 = 0$ and simulating the model with the parameter values in Table 3. Figures 8, 9, and 10 show a graphic illustration of the impact of FCM on the susceptible host without intervention. Figure 8 shows a 30-day graph of susceptible hosts versus time. According to Figure 8, the susceptible population expands logistically from 100 to 428 people. Because the carrying capacity of the susceptible host is set at 1000, the presence of the FCM pest causes the susceptible host to grow below its carrying capacity. Due to the effect of FCM on the susceptible host population, when the initial population increases to 500, the susceptible host population drops exponentially and then levels off at 428.

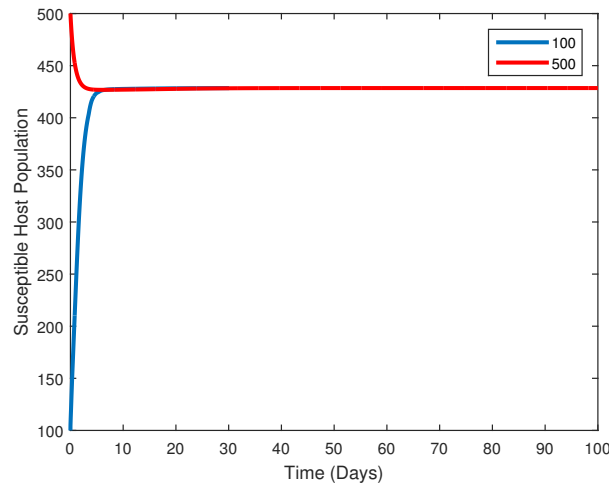


Figure 8: A plot of a susceptible host against time without control

Figure 9 shows a graph of the total population of FCM overtime for 30 days. According to Figure 9, the population of FCM first increases dramatically from 1000 to a maximum value, then gradually decreases, then increases again, and drops slightly below 1000 after 100 days. The first increase is due to the increased availability of food from FCM pests. As time passes, the number of susceptible hosts available begins to decline, resulting in a decrease. As more susceptible hosts are introduced into the population and the polyphagous nature of FCM, FCM naturally coexists near 1000.

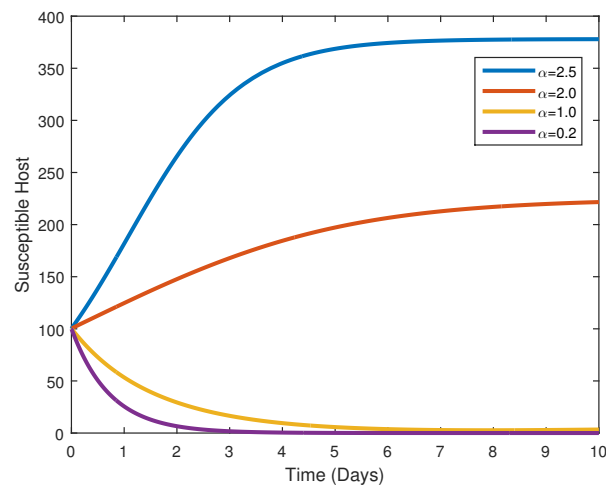


Figure 9: A plot of the total population of FCM with time in the presence of FCM without control

Figure 10 represents a graph of a susceptible host with time in the presence of FCM in the absence of any control when $\alpha = 1.2$ while maintaining the other parameters in Table 1 constant. Figure 9 shows that the number of susceptible hosts decreases with time from 100 to 0. This shows that, in the absence of any control measure of FCM, the FCM feeds on the available hosts until the population is completely depleted.

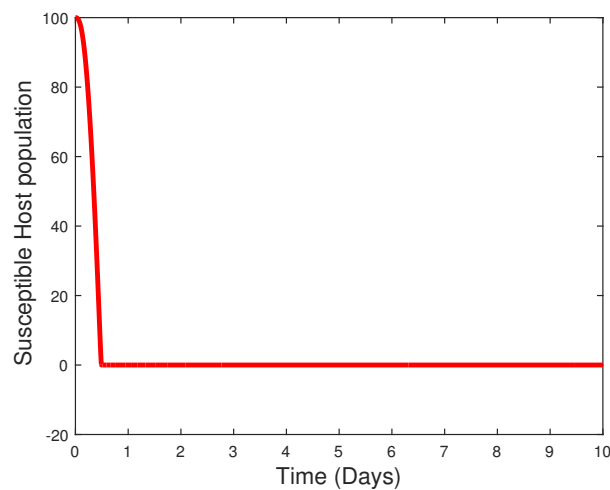


Figure 10: A plot of the susceptible host with time in the presence of the FCM without control

The presence of FCM in the population leads to a decrease in the susceptible host population. As the host population reduces the FCM in the larval stage, its population also declines, as illustrated by the numerical simulation in Figure 9. Therefore, the presence of FCM on the farm has more significant economic effects and reduces crop yields. These

findings are in agreement with those of [40]. Therefore, it is essential to employ control measures to eliminate FCM.

4.2.3. Impact of Sterile Insect on FCM Control

To explore the impact of sterilised insects on the FCM population, the system model 1 is numerically analysed with the parameter values in Figure 1. Figure 11 shows a graph of the population of FCM over time, with a sterile release rate of $\psi = 100$ in 20 days. In Figure 10, the number of FCM first decreases, then starts to increase to about 450, then gradually drops to zero as time increases. This indicates the effectiveness of sterile insect release as an FCM biological control method.

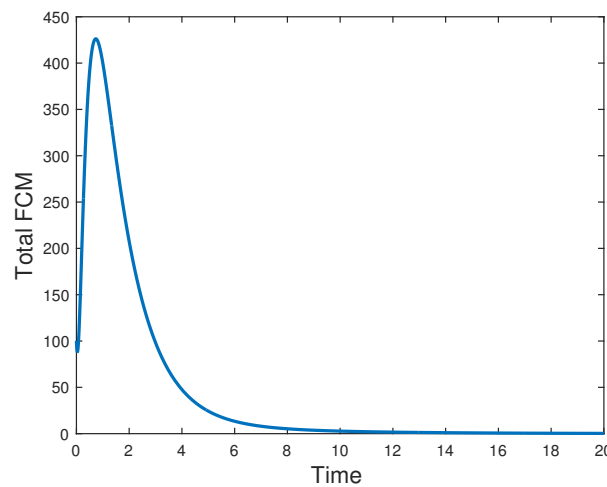


Figure 11: A plot of FCM Population against Time (Days)

Figure 12 illustrates a graph of the sterile insect population compared to the FCM population for 20 days. In Figure 12, it is observed that the number of FCM decreases slightly first, then increases to approximately 450, then gradually decreases to zero, when the sterile insect is approximately 120. Therefore, sterile insects help reduce the number of FCM by making fertile females infertile through mating and only capable of producing infertile eggs, thus helping to reduce the population of FCM.

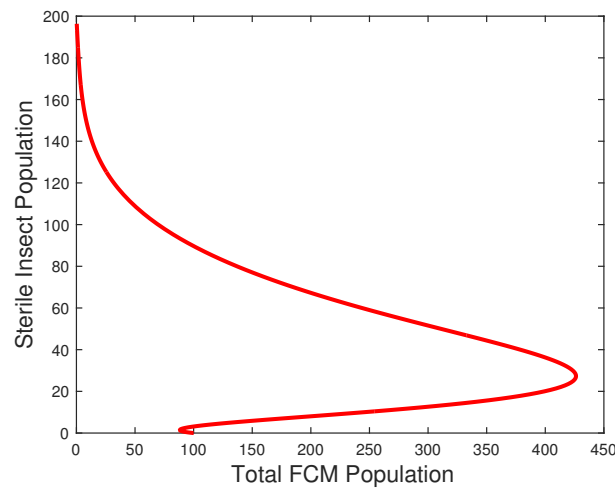


Figure 12: A plot of sterile insect release against the FCM population

The impact of sterile insect release on the susceptible host population is obtained by setting the pheromone compartment in model system 1 to zero that is setting $\nu = 0, \nu = 0$, then simulating the model using same initial condition for a period between 0 to 100 days at 20°C temperature. The impact of sterile insect on the host and FCM is illustrated in Figures 13, 14, 15 and 16. Figure 13 shows a plot of the number of sterile against time within a period of 10 days, 30 days and 100 days, with initial value of sterile insect set at zero and release rate $\psi = 100$. From the graph its observed that the number of sterile insect increase gradually up to a maximum value with time and follows the same trajectory at all times. Any further increase in time does not require additional increase in the sterile insect.

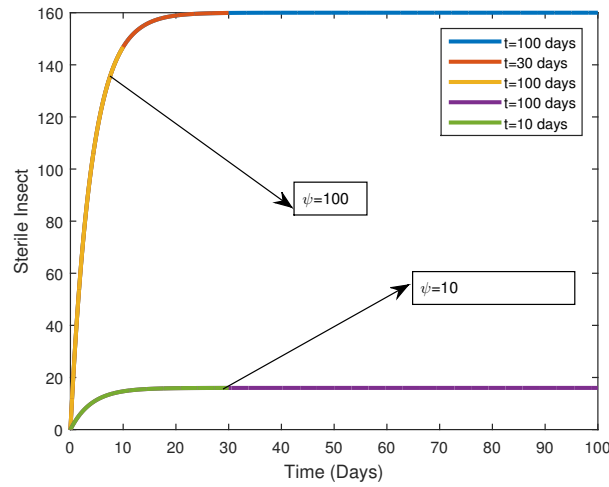


Figure 13: A plot of Number of Sterile Insect Release with Time

Figure 14 shows a plot of Susceptible host against sterile insect as a control measure of FCM, with the initial number of sterile insect set at zero and the release rate per day varied from 5, 10, and 100 sterile release per day. The susceptible host carrying capacity is set constant at $K_h = 1000$. From the graph it is evident that the minimum number of sterile release rate that would bring the susceptible host to its carrying capacity is approximately 5 sterile insect per day; any further increase in the sterile insect would have no effect on the yields of susceptible host. This shows that sterile insect techniques help control the FCM population from the farm hence leading to high yields.

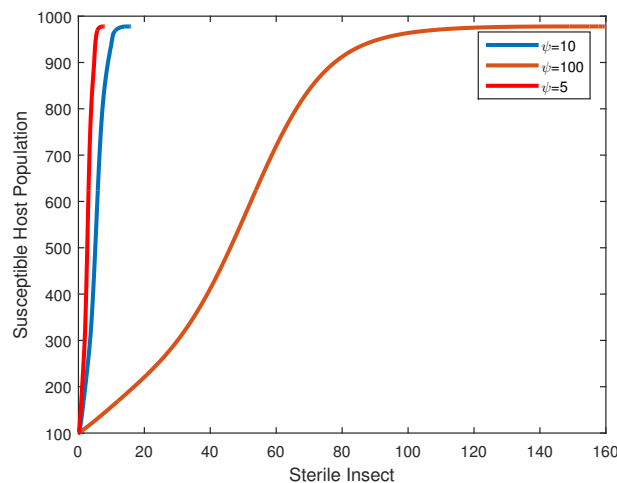


Figure 14: A plot of Susceptible Host against the Sterile Insect Release in the absence of Pheromone Traps

Figure 15 shows a plot of the total FCM population against the number of sterile insect released in the field under various release rate per day within a period of 30 days while keeping other parameters as indicated in Table 1. From the graph its observed that the population of FCM first increases from the initial population to a maximum and gradually drops to zero. The 10 sterile insect release per day is found to be more effect than 100 sterile insect release per day. This shows the impact of sterile insect on the reduction of the population of FCM as a biological control measure.

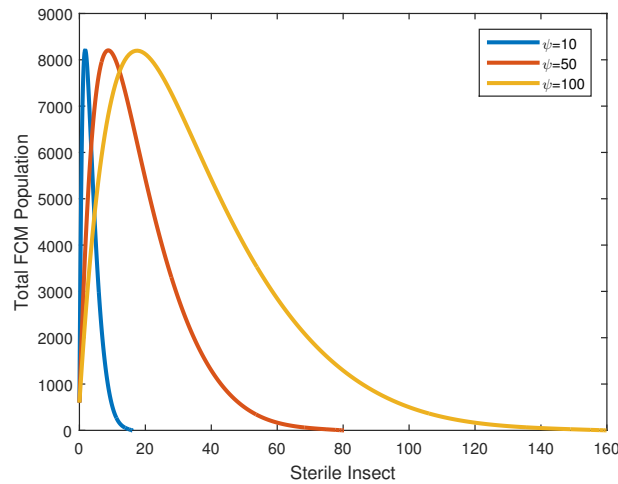


Figure 15: A plot of Total FCM Population against Sterile Insect Release in the absence of Pheromone Traps

Figure 16 shows a plot of a dult FCM population against the sterile insect, with the sterile release rate $\psi = 100$ within a period of 30 days. From the Figure the number of a dult FCM decreases from the initial values of 100 in each compartment to 0. This indicates the effectiveness of sterile insect release as an FCM biological control method.

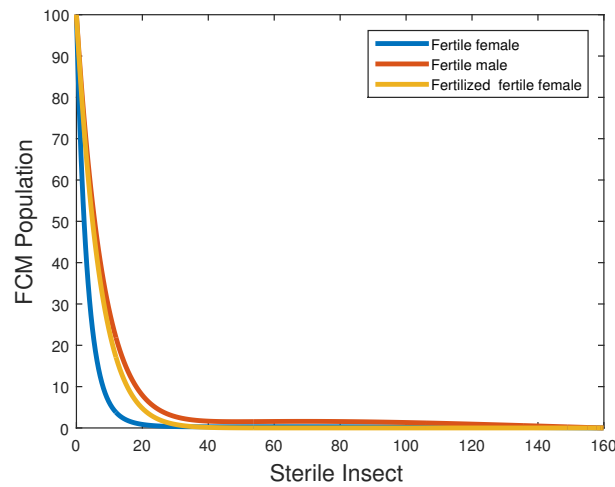


Figure 16: A plot Adult FCM Population against Sterile Insect Release

Figure 17 illustrate a plot of fertilized fertile female population against sterile insect under different release rates that is when $\psi = 100$, $\psi = 50$ and $\psi = 10$. From the Figure it is observed that the number of fertilized fertile female decreases from the initial population of 100 gradually to near zero with the increase in sterile insect and remain constant at near zero. Higher release rate does not provide a faster control as illustrated in Figure 10. Sterile insect therefore help in reducing the number of fertilized fertile female by making the fertile female infertile through mating and only able to produce infertile eggs, hence helps in reducing the population of FCM.

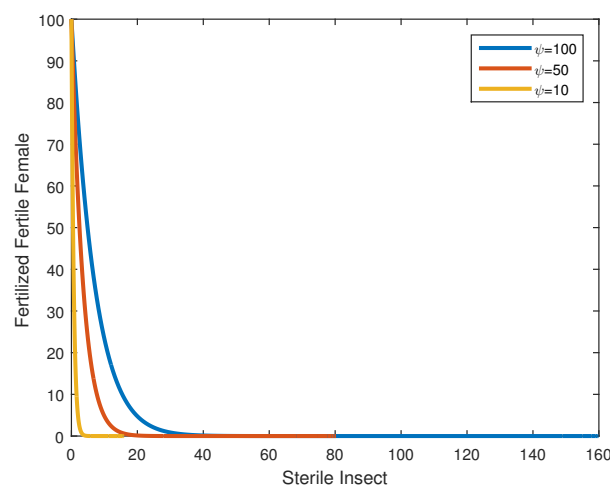


Figure 17: A plot of Fertilized Fertile Female against Sterile Insect Release

The impact of sterile insect release on the susceptible host population is obtained by setting the pheromone compartment in model system 1 to zero, that is, setting $nu = 0, v = 0$, then simulating the model for a period between 0 and 100 days at a temperature of 200C. The impact of a sterile insect on the host is illustrated in Figures 18 and 19: Figure 18 shows a graph of the number of susceptible hosts over time in 10 days, 20 days, with the sterile insect technique as the FCM control agent. According to Figure 18, the population of susceptible hosts gradually increases to carry capacity.

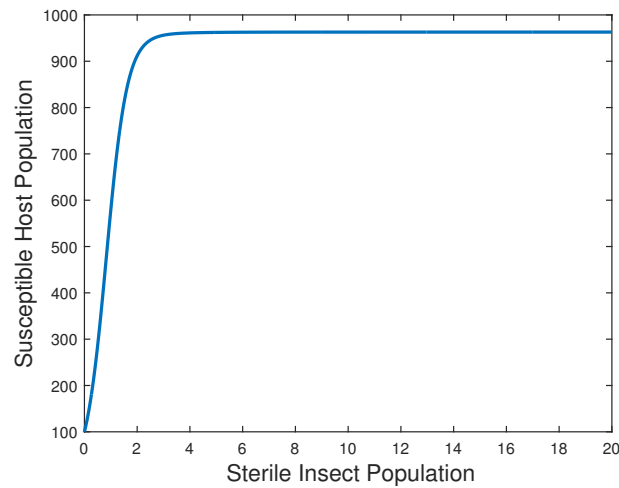


Figure 18: A plot of a susceptible host with time in the SIT

Figure 19 illustrates a graph of susceptible hosts versus sterile insects as an FCM control measure, with the initial number of sterile insects set to zero and the release rate per day at 100. The carrying capacity of the susceptible host is set at $K_h = 1000$. In Figure 19, it is observed that the population of susceptible hosts increases in carrying capacity as the population of sterile insects increases. Any further increase in the sterile insect would not affect the yields of the susceptible host. This shows that sterile insect techniques help increase crop yields on the farm.

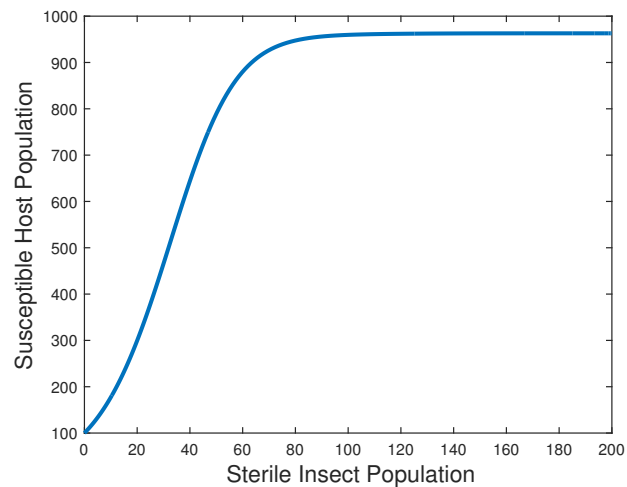


Figure 19: A plot of the susceptible host against the sterile insect population

Insect populations can be controlled by the release of large numbers of sterile males. Therefore, if a fertile female mates with a sterile male, the female will lay non-hatching eggs. Analysis of the host-parasite interaction model in the presence of sterile insects shows that to reduce FCM infestation, sterile insects should be released into the population within the values of the threshold parameter. The value of the practical parameter of the sterile insect release rate reduces the larval conversion rate and its attack rate, which, in turn, reduces the value of the basic reproduction number to less than unity, and thus is very effective in controlling the FCM infestation. When many sterile males are released in the field, the local population of FCM tends to decline or disappears with time. Numerical simulation showed that in the presence of SIT, FCM control is an effective biological method of controlling FCM infestation in the susceptible host population.

The study revealed that the control of FCM using the sterile insect method is effective, provided that the number of sterile releases is above the threshold value. Furthermore, the study reveals that the success of sterile release depends on the entomological parameters of the FCM, as well as the parameters of the sterile male, which determine the threshold value.

5. Conclusion

Pest control has advanced significantly in recent years as it has become clear that pesticides alone are frequently insufficient, if not harmful, for many pest problems, particularly in FCM. An adequate understanding of the biological dynamics associated with pest control techniques is becoming increasingly clear in any pest control programme.

In this study, a deterministic mathematical model of sterile insect technique is developed for control of false codling moth. Although some researchers, such as [3] and [2], have developed biological pest control models, none of these models have taken into account the host compartment. Furthermore, most of these models have focused on general pest control rather than specific pest species, and some of the models have only captured pest dynamics while ignoring crop population, which has a significant impact on crop and pest interactions. Keeping pest densities below economic thresholds is one of the most important aspects of pest control. These levels are closely related to the crop population's dynamic evolution. As a result, we incorporated the dynamic of susceptible host population, FCM age-structured compartments into model system 1.

We carefully examined the model and determined three ecological equilibrium points for the system model. i) pest-free equilibrium point (E_0); ii) co-existence equilibrium point (E_1); and iii) host-free equilibrium point (E_2). Due to its triviality, the host-free equilibrium has not been subjected to stability analysis. The primary objective of this study is to determine the values of the threshold parameter of the sterile release rate that will cause the extinction of FCM, thus ensuring the survival of susceptible hosts.

Based on our analytical and numerical analysis of the system model, we determined a critical value of the sterile insect release rate, beyond which the FCM will become extinct. We also validated this discovery using numerical simulation. The model analysis revealed that there is a domain in which the model is well posed entomologically and mathematically. The system's basic reproduction numbers were calculated using the next-generation matrix. When a critical release value of the sterile release rate is met, the numerical simulation of the model shows that sterile release is an effective way to control the FCM population.

6. Acknowledgements

We thank the administrative staff of the Department of Physical Sciences of Chuka University for their hospitality and assistance with matters related to our research work.

References

- [1] Abuasbeh, K., Qureshi, S., Soomro, A., and Awadalla, M. (2023). An optimal family of block techniques to solve models of infectious diseases: Fixed and adaptive stepsize strategies. *Mathematics*, 11(5):1135.
- [2] Anguelov, R., Dufourd, C., and Dumont, Y. (2017). Mathematical model for pest–insect control using mating disruption and trapping. *Applied Mathematical Modelling*, 52:437–457.
- [3] Anguelov, R., Dumont, Y., and Lubuma, J. (2012). Mathematical modeling of sterile insect technology for control of anopheles mosquito. *Computers & Mathematics with Applications*, 64(3):374–389.
- [4] Barclay, H. J. (2016). Determination of the sterile release rate for stopping growing age-structured populations. *International Journal of Pest Management*, 62(1):40–54.
- [5] Barros-Parada, W., Knight, A. L., and Fuentes-Contreras, E. (2015). Modeling codling moth (Lepidoptera: Tortricidae) phenology and predicting egg hatch in apple orchards of the Maule region, Chile. *Chilean journal of agricultural research*, 75(1):57–62.
- [6] Ben Dhahbi, A., Chargui, Y., Boulaaras, S. M., Ben Khalifa, S., Koko, W., and Alresheedi, F. (2020). Mathematical modelling of the sterile insect technique using different release strategies. *Mathematical Problems in Engineering*, 2020.

- [7] Bhunu, C. and Mushayabasa, S. (2011). Modelling the transmission dynamics of pox-like infections. *IAENG International Journal*.
- [8] Bloem, S., Carpenter, J. E., and Hofmeyr, J. H. (2003). Radiation biology and inherited sterility in false codling moth (lepidoptera: Tortricidae). *Journal of Economic Entomology*, 96(6):1724–1731.
- [9] Blomefield, T. (1989). Economic importance of false codling moth, cryptophlebia leucotreta, and codling moth, cydia pomonella, on peaches, nectarines and plums. *Phytophylactica*, 21(4):435–436.
- [10] Blomefield, T. et al. (1989). Economic Importance of False Codling Moth, Cryptophlebia leucotreta, and Codling Moth, Cydia Pomonella, on Peaches, Nectarines and Plums. *Phytophylactica*, 21(4):435–436.
- [11] Carde, R. T. (1990). Principles of mating disruption. *Behavior-Modifying Chemicals for Insects Management: Applications of Pheromones and Other Attractants*.
- [12] Carpenter, J. E., Bloem, S., and Hofmeyr, J. H. (2004). Acceptability and suitability of eggs of false codling moth (lepidoptera: Tortricidae) from irradiated parents to parasitism by trichogrammatoidea cryptophlebiae (hymenoptera: Trichogrammatidae). *Biological Control*, 30(2):351–359.
- [13] Castillo-Chavez, C. and Song, B. (2004). Dynamical models of tuberculosis and their applications. *Mathematical Biosciences & Engineering*, 1(2):361.
- [14] Dufourd, C. and Dumont, Y. (2012). Modeling and simulations of mosquito dispersal. the case of aedes albopictus. *Biomath*, 1(2):1209262.
- [15] Dyck, V. A., Hendrichs, J., and Robinson, A. S. (2021). *Sterile insect technique: principles and practice in area-wide integrated pest management*. Taylor & Francis.
- [16] Garcia, A. G., Godoy, W. A., Cônsoli, F. L., and Ferreira, C. P. (2020). Modelling movement and stage-specific habitat preferences of a polyphagous insect pest. *Movement Ecology*, 8(1):1–11.
- [17] Georgescu, P., Hsieh, Y.-H., and Zhang, H. (2010). A lyapunov functional for a stage-structured predator–prey model with nonlinear predation rate. *Nonlinear Analysis: Real World Applications*, 11(5):3653–3665.
- [18] Gianni, G., Pasquali, S., Parisi, S., and Winter, S. (2014). Modelling the Potential Distribution of Bemisia Tabaci in Europe in Light of the Climate Change scenario. *Pest Management science*, 70:1611–1623.
- [19] Gilligan, T. M., Epstein, M. E., and Hoffman, K. M. (2011). Discovery of false codling moth, thaumatotibia leucotreta (meyrick), in california (lepidoptera: Tortricidae). *Proceedings of the Entomological Society of Washington*, 113(4):426–435.
- [20] Hofmeyr, J. H., Hofmeyr, M., Lee, M., Kong, H., and Holtzhausen, M. (1998). Assessment of a cold treatment for the disinfestations of export citrus from false codling moth, thaumatotibia leucotreta (lepidoptera: Tortricidae): a report to the people's republic of china. *Citrus Research International* <http://www.citrusres.com/sites/default/files/documents/FCM%20cold%20disinfestation%20study%20for%20Korea,201998>.
- [21] Jimrise, O., Okongo, M. O., and Muraya, M. (2021). Mathematical modeling of host - pest interactions in stage-structured populations: A case of false codling moth [thaumatotibia leucotreta]. *Journal of Progressive Research in Mathematics*, 18(4):1–21.
- [22] Jimrise Ochwach, Mark O. Okongo, M. M. (2021). Mathematical model for false codling moth control using pheromone traps. *International Journal of Applied Mathematical Research*, 10(2):32–52.
- [23] Kalajdzievska, D. (2007). *Modeling the Effects of Carriers on the Transmissions Dynamics of Infectious Diseases*. PhD thesis, University of Alberta.
- [24] Korobeinikov, A. and Wake, G. C. (2002). Lyapunov functions and global stability for sir, sirs, and sis epidemiological models. *Applied Mathematics Letters*, 15(8):955–960.
- [25] La Salle, J. P. (1966). An invariance principle in the theory of stability. Technical report.
- [26] McCluskey, C. C. (2010). Complete global stability for an sir epidemic model with delay—distributed or discrete. *Nonlinear Analysis: Real World Applications*, 11(1):55–59.
- [27] Mkiga, A., Mohamed, S., du Plessis, H., Khamis, F., and Ekesi, S. (2019). Field and Laboratory Performance of False Codling Moth, Thaumatotibia Leucotreta (Lepidoptera: Tortricidae) on Orange and Selected Vegetables. *Insects*, 10(3):63.
- [28] Moore, S. (2012). Moths and Butterflies: False Codling Moth. *Citrus Research International IPM Production Guidelines*, 3(Part 9.4).
- [29] Murray, J. (2002). Mathematical biology (eds antman, ss, marsden, je, sirovich, l. & wiggins, s.) 175–256.
- [30] Myburgh, M. et al. (1969). Effect of Low Temperature Storage on Pupae of False Codling Moth, Cryptophlebia (Argyroplote) leucotreta Meyr. *Phytophylactica*, 1(3_4):115–116.
- [31] Pasquali, S., Soresina, C., and Gilioli, G. (2019). The effects of fecundity, mortality and distribution of

- the initial condition in phenological models. *Ecological modelling*, 402:45–58.
- [32] Peshin, R. and Dhawan, A. K. (2009). *Integrated Pest Management: Volume 1: Innovation-Development Process*, volume 1. Springer Science & Business Media.
 - [33] Qureshi, S., Ramos, H., Soomro, A., and Hincal, E. (2022). Time-efficient reformulation of the lobatto iii family of order eight. *Journal of Computational Science*, 63:101792.
 - [34] Ramos, H., Qureshi, S., and Soomro, A. (2021). Adaptive step-size approach for simpson's-type block methods with time efficiency and order stars. *Computational and Applied Mathematics*, 40(6):219.
 - [35] Savary, S., Teng, P. S., Willocquet, L., and Nutter Jr, F. W. (2006a). Quantification and modeling of crop losses: a review of purposes. *Annu. Rev. Phytopathol.*, 44:89–112.
 - [36] Savary, S., Teng, P. S., Willocquet, L., and Nutter Jr, F. W. (2006b). Quantification and Modeling of Crop Losses: A Review of Purposes. *Annu. Rev. Phytopathol.*, 44:89–112.
 - [37] Sergio, R. (2014). The optimal release of sterile males in pest management. *All Graduate Plan B and other Reports*, 408:128.
 - [38] Steiner, L. F., Harris, E., Mitchell, W. C., Fujimoto, M., and Christenson, L. (1965). Melon fly eradication by overflooding with sterile flies. *Journal of Economic Entomology*, 58(3):519–522.
 - [39] Stibick, J., Bloem, S., Carpenter, J., Ellis, S., and Gilligan, T. (2008a). New Pest Response Guidelines: False Codling Moth *Thaumatotibia leucotreta*. Technical report, USDA-APHIS-PPQ-Emergency and Domestic Programs, Riverdale, Maryland. [http](http://...)
 - [40] Stibick, J., Bloem, S., Carpenter, J., Ellis, S., Gilligan, T., Usnick, S., and Venette, R. (2008b). New pest response guidelines: false codling moth *thaumatotibia leucotreta*. Technical report, USDA-APHIS-PPQ-Emergency and Domestic Programs, Riverdale, Maryland. [http](http://...)
 - [41] Wester, T. (2015). Analysis and simulation of a mathematical model of ebola virus dynamics in vivo. *Society for Industrial and Applied Mathematics*, 8:236–256.